J. Membrane Biol 72, 17–41 (1983)

The Journal of
Membrane Biology

Topical Review

Impedance Analysis in Epithelia and the Problem of Gastric Acid Secretion

Jared M. Diamond* and Terry E. Machen†

* Department of Physiology, University of California Medical Center, Los Angeles, California 90024, and
† Department of Physiology and Anatomy, University of California, Berkeley, California 94720

Introduction

The electrophysiological technique of impedance analysis has much potential value in studies of epithelia. In addition to offering advantages over cable analysis as a means of resolving junctional, apical, and basolateral resistances, it provides a method for measuring membrane areas and configurations nondestructively in the living tissue, without the fixation artifacts and sampling problems inherent in electron microscopy. It is not that we expect epithelial electron microscopists to be put out of business by impedance analysis, which has artifacts and technical difficulties of its own. Rather, we see impedance analysis as a useful method for integrating physiological and ultrastructural findings in some cases.

Although impedance studies of epithelia began as long ago as 1945 and at least 15 papers have been published on the subject, the method has not ranked among the major avenues to understanding of epithelia, and its potential has remained unfulfilled. We see two reasons for this outcome. First, it is only recently that six key problems in its application to epithelia have been attacked or overcome: the development of circuit models incorporating distributed resistors; understanding of the short-comings of transient (square-wave) analysis, especially for circuits with distributed resistors; development of better techniques for rapid impedance analysis; the abandonment of data representation by Nyquist plots, which are less sensitive to effects of model parameters than are Bode plots; development of techniques for impedance analysis of leaky epithelia; and development of methods for intracellular impedance analysis. Second, impedance analysis, like other difficult electrophysiological techniques, has sometimes seduced investigators into asking questions within the formalism erected by the analysis itself, instead of translating the formalism and using the analysis to answer biologically significant questions. The significant questions are not "Why does the locus of the Nyquist plot deviate from a single semicircle, and why does its center lie off the real axis, and why does α for the phase-shift element differ from one?" but instead "How is the epithelium organized, and what happens during the onset of transport?"

Most epithelial impedance measurements to date have been performed on gastric mucosa, an exceptionally complicated epithelium whose understanding has depended as much on ultrastructural and biochemical techniques as on electrophysiological techniques. This review therefore takes the shape of a boa constrictor that has just swallowed a large pig (Fig. 1, based on experimental observations by Wyss 1814, and on Figs. 1–3 of Saint-Exupéry, 1943). After this introduction, we devote half of the review to the problems raised by ultrastructural, biochemical, and electrophysiological studies of gastric mucosa. We then discuss in turn the potential uses of impedance analysis in epithelia; its theory and practice; epithelial impedance studies to data; and how, particularly, impedance studies have been used to clarify the surprisingly low transepithelial resistance of gas-

Key words acid secretion · circuit analysis · distributed resistor · gastric mucosa · impedance analysis · stomach

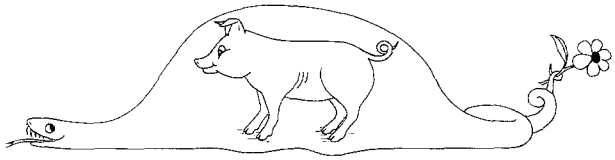

Fig. 1.

tric mucosa, its change with acid secretion, and its relation to epithelial ultrastructure. Finally, we outline for gastric mucosa and other epithelia some of the unanswered questions to whose solution impedance analysis could make decisive contributions in the future. Readers interested in gastric mucosa but not in impedance analysis itself may skip pp. 32–34. Readers interested in impedance analysis but not specifically in gastric mucosa may skip pp. 25–28.

Gastric mucosa

Stimulation of gastric mucosa induces many complex and spectacular changes within the oxyntic (acid secreting) cells: changes in H^+, Cl^-, and water secretion, in permeability and conductance to ions, and in ultrastructure. Because gastric mucosa exhibits such a wide range of activities, it has interested experimentalists from numerous disciplines. With the advent of electrophysiological and isotopic tracer techniques, physiologists studied the changes in transepithelial PD, resistance, and ionic fluxes that accompanied stimulation of acid secretion. More recently, the electron microscope allowed anatomists to study the accompanying dramatic ultrastructural changes. Within the past 10–15 years biochemical techniques have also come into play, notably in studying transport and permeability characteristics of membranes isolated from the apical aspects of oxyntic cells.

While it has been obviously beneficial to approach the general problem of acid secretion from these several perspectives, it becomes essential to find ways of integrating this information. Impedance analysis recommends itself as one such method, especially for integrating electrophysiological and ultrastructural information. Our overview of the phenomena requiring integration starts with a brief summary of events accompanying the onset of acid secretion, and proceeds to more detailed consideration of the ultrastructural changes and the basic electrophysiology. We then describe the insights into the H^+ secretion "pump" provided by biochemical and vesicle studies of isolated oxyntic cell membranes. (For a detailed account of this field *see* the recent review by Sachs, Faller, and Rabon, 1982). Finally, we examine the mechanisms of the major ion transport processes in gastric mucosa. Our review omits consideration of the organic components of gastric juice (mucus and enzymes), as little is known about the relationship between their secretion and ion secretion.

Sequence of Events during Stimulation of Acid Secretion

Figure 2 illustrates, for frog gastric mucosa *in vitro*, the large electrophysiological changes following addition of histamine, the most potent stimulant of acid secretion. Transepithelial resistance always decreases greatly, from starting values of hundreds of $\Omega\,cm^2$ to as little as 20–70 $\Omega\,cm^2$ (Forte & Machen, 1975; McLennan, Machen & Zeuthen, 1981; N. Raphael & T. Machen, *unpublished observations*). These resistance values for stimulated gastric mucosa are in the range of those observed for epithelia with "leaky" junctions, such as gallbladder and small intestine (Frömter & Diamond, 1972). H^+ secretion appears a few minutes after the start of the resistance drop and rises to 5–7 $\mu eq/cm^2$ hr in frog stomach and up to 300 $\mu eq/cm^2$ hr in intact mammalian stomach (*compare* the Na^+ absorption rate of 1–3 $\mu eq/cm^2$ hr for frog skin or toad bladder to appreciate why the word "dramatic" cannot be avoided in discussions of gastric acid secretion).

Soon after resistance begins to drop, the mucosa-negative transepithelial PD increases (Fig. 2). This small, consistent increase in PD is followed by a large but variable decrease, whose magnitude depends on the species[1] and on the magnitude of the drop in resistance. The drop in resistance partly accounts for the drop in PD, but the two changes are not directly proportional because short-circuit current I_{sc} also changes. The I_{sc} causing the mucosa-negative PD has two main components: an excess of active Cl^- secretion over H^+ secretion (Hogben 1955; Machen & McLennan, 1980; Forte & Machen, 1983); and, in mammals (Forte & Machen, 1975; Tripathi & Rangachari, 1980) and reptiles (Hansen, Slegers & Bonting, 1975) but not frogs, active absorption of Na^+. Because rates of Cl^- secretion and Na^+ absorption vary among species and appear to be influenced to different degrees by histamine stimulation (Machen & Forte, 1979), it is not surprising that the PD response of stimulated gastric mucosa is somewhat variable.

The other ionic transport processes appear to be either electroneutral or else quantitatively small. The H^+ secretion mechanism itself appears to be a neutral H^+-K^+ exchange pump (Sachs et al., 1976; Lee, Breitbart, Berman & Forte, 1979) that

[1] In frog and toad stomach the steady-state PD is usually lower in stimulated than in resting tissues. The reverse is true for piglet stomach. In dogfish stomach the PD is normally very low and reversed in orientation (mucosal solution a few mV positive to serosal solution), and stimulation-induced PD changes are also very small (Hogben, 1959).

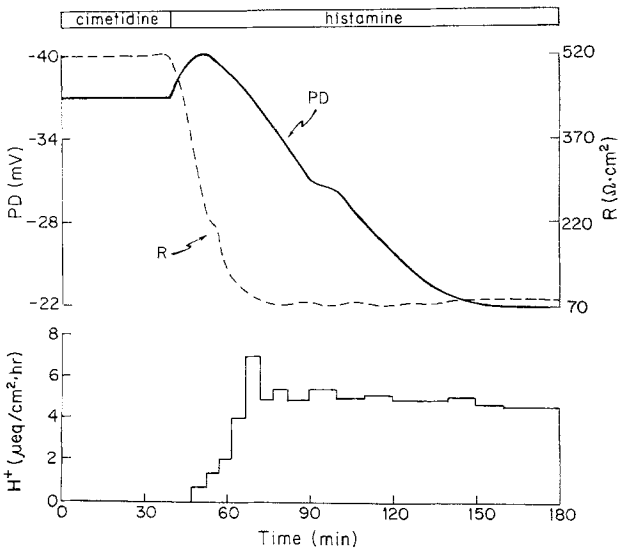

Fig. 2. Time course of activation of H^+ secretion and of changes in transepithelial resistance and PD (mucosal solution with respect to serosal solution), following histamine stimulation, in frog gastric mucosa. The tissue was mounted in Ussing chambers and initially incubated in the presence of the histamine (H_2) antagonist cimetidine at 10^{-4} M. The cimetidine was then removed and replaced with 10^{-4} histamine added to the serosal solution. Note that PD and resistance change immediately but that the onset of H^+ secretion is delayed by ~6–7 min

does not contribute *directly* to the generation of the PD, at least in normal Cl^- and HCO_3^--containing solutions (but *see* Rehm & Sanders, 1977).[2] In addition, during H^+ secretion an OH^- ion is left behind inside the cell and neutralized there to HCO_3^- by combining with CO_2 from metabolism and from the serosal (or blood) solution (Davies, 1948). This reaction is probably catalyzed by carbonic anhydrase (Davies, 1948). The HCO_3^- then exits the cell into the serosal solution via Cl^--HCO_3^- exchange at the serosal membrane, another neutral process (Rehm & Sanders, 1975). In addition to these well-known major secretory processes in the oxyntic cells, it has recently been found that the other major cell type of gastric mucosa, the surface epithelial cells, can secrete HCO_3^- at about 10% of the rate of H^+ or Cl^- secretion by the oxyntic cells (Flemstrom 1977; Flemstrom & Garner, 1982). This HCO_3^- helps maintain neutral pH in the unstirred layer near the surface cells, and thereby protects them from being damaged by the acid produced by their dangerous neighbors, the oxyntic cells (Ross, Baharai & Turnberg, 1981). As the rate of HCO_3^- secretion is low, the question whether it contributes to electrical characteristics of gastric mucosa remains unresolved [*compare* Flemström (1977) with Takeuchi and Silen (1982)].

Simultaneously with these large changes in resistance and PD, the oxyntic cells of both mammals and amphibia undergo striking ultrastructural changes. Resting cells have short microvilli at their apical surface, and the cytoplasm is filled with smooth membranes in the form of tubules and vesicles (Figs. 3–5 and 9a). Stimulated cells exhibit an increase in apical membrane surface area by at least six- to 10-fold and a concomitant depletion of intracellular smooth membrane (Figs. 6–8 and 9*b*, Table 1). The nature of the transition between these two states that are so distinct from each other morphologically is controversial.

Because the onset of H^+ secretion, the decrease in resistance and PD, and the increase in apical membrane area all occur at approximately the same time, one might reasonably suppose that these events are intimately related to each other. As we shall see, impedance analysis has contributed importantly to clarifying these relations.

The Process of Membrane Elaboration

Gastric mucosa is enormously folded at many levels. At the grossest level, the whole epithelium is thrown into elaborate folds (rugae) that increase the actual area over nominal surface area several times. The rugae are further indented into pits, which split further into four or five branches called gastric glands (Helander, 1981). The second- and third-level folding represented by the pits and glands increases the actual area by a further factor of 13 (Blum et al., 1971; Helander & Hirschowitz, 1972; Helander et al., 1972; Helander, 1981). Mucus-secreting surface epithelial cells cover the areas of the stomach wall in direct contact with the lumen, and they extend part of the way down the gastric pits. Acid and enzyme secretion takes place in the glands, in separate enzyme-secreting (chief) and acid-secreting (oxyntic) cells in mammals but together in a single cell type in lower vertebrates. Readers interested in the detailed histology of the stomach are referred to the excellent review by Helander (1981).

Yet a fourth level of folding is provided within the oxyntic cells, both in mammals and in lower vertebrates. In the resting state (frog, Figs. 3–5; piglet, Fig. 9a) transmission and scanning electron micrographs show the apical membrane of the oxyntic cells to be covered with short, stubby microvilli. The apical cytoplasm is full of membranes,

[2] In Cl^--free solutions frog gastric mucosa exhibits a reversed short-circuit current that apparently does represent H^+ transport (Heinz & Durbin, 1959; Rehm & Sanders, 1977).

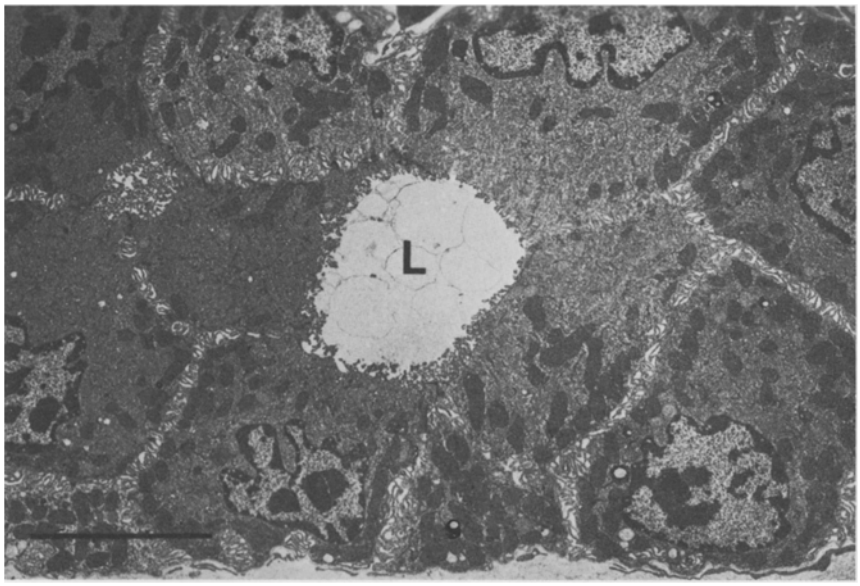

Fig. 3. Low-magnification (× 2,400) transmission electron micrograph (TEM) of a cross-section of bullfrog resting gastric mucosa, *in vitro*. Several oxyntic cells surround the lumen (*L*) of a gastric gland. Bar = 10 μm. (From Logsdon and Machen, 1982*b*, reproduced from The Anatomical Record, published for the Wistar Press by Alan R. Liss, Inc.)

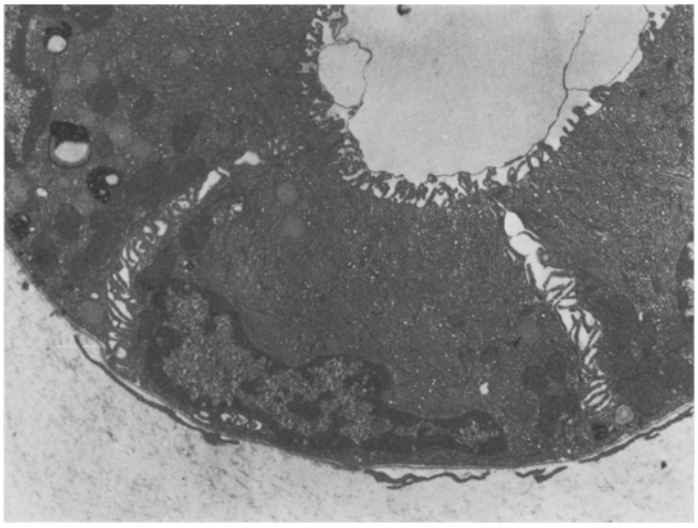

Fig. 4. Higher-power (× 5,000) TEM of oxyntic cell from bullfrog resting gastric mucosa. The cell's apical surface, which faces the lumen at upper right, is covered with short microvilli. The apical cytoplasm is filled with tubules, some of which are cut in cross-section and appear as vesicles. (From Logsdon and Machen, 1982*b*, reproduced from The Anatomical Record, published for the Wistar Press by Alan R. Liss, Inc.)

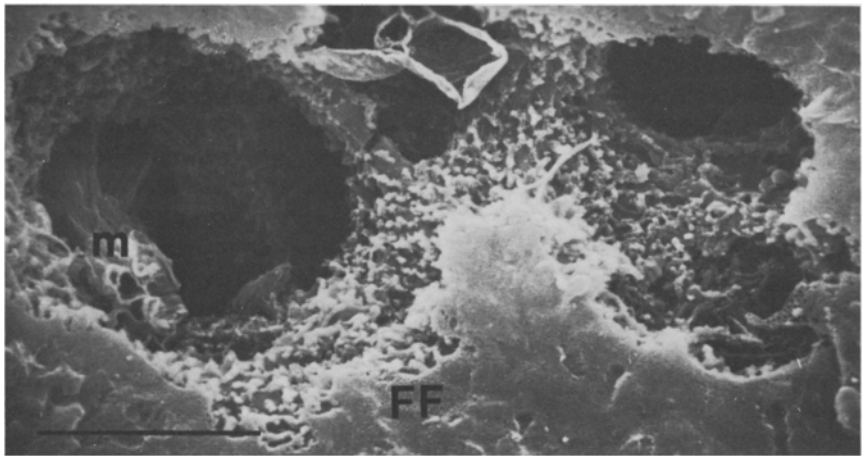

Fig. 5. Scanning electron micrograph of the same tissue as in Fig. 3. Cryofracture has exposed a portion of the gastric gland. The lumen contains some mucus (*m*). The fracture face (*FF*) shows few details at this magnification. This SEM view confirms that the exposed oxyntic cells are covered with short, stubby microvilli. Bar = 10 μm. (From Logsdon and Machen, 1982*b*, reproduced from The Anatomical Record, published for the Wistar Press by Alan R. Liss, Inc.)

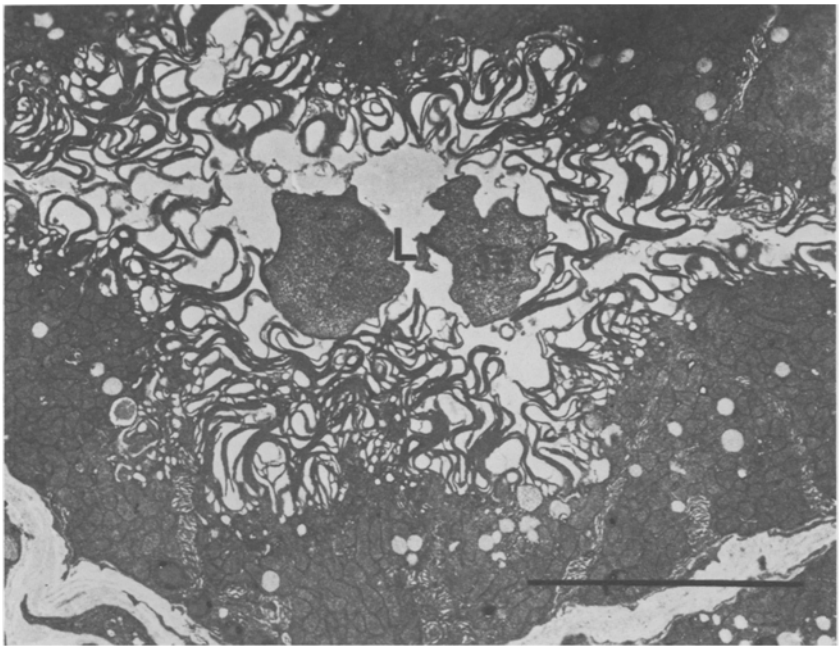

Fig. 6. Cross section of gastric gland from bullfrog gastric mucosa *in vitro*, stimulated by histamine plus dbcAMP and the potent phosphodiesterase inhibitor IBMX to minimize secretory responses. Long cellular projections fill the lumen. Bar = 10 μm. × 3,700. (From Logsdon and Machen, 1982*b*, reproduced from The Anatomical Record, published for the Wistar Press by Alan R. Liss, Inc.)

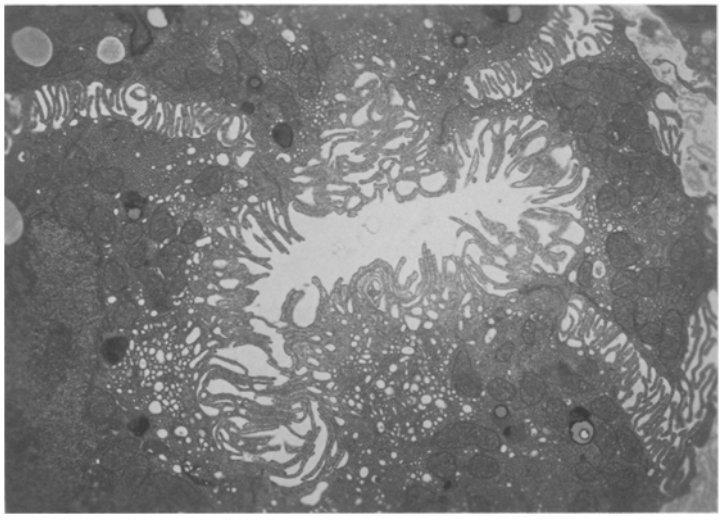

Fig. 7. Higher-power TEM (× 6,000) of oxyntic cell from bullfrog stimulated gastric mucosa. Note that the apical membrane is enormously elaborated and that fewer tubules remain in the apical cytoplasm. Also note the interdigitations of folded lateral membranes. (From Logsdon and Machen, 1982*a*)

of which in the frog some obviously have the form of tubules while others appear as vesicles (Fig. 4). However, freeze-fracture replicas show that the "vesicles" are simply tubules cut in a cross section (Forte & Forte, 1971). In mammals the intracellular membranes have the form of vesicles in chemically fixed cells (Fig. 9*a*; *see also* Forte et al., 1982), but recent studies from Ito's laboratory by a rapid freezing technique suggest that these membranes are actually similar to the intracellular tubules of the frog (S. Ito, *personal communication*). However, the apical *surface* of the mammalian oxyntic cell is folded into intracellular canaliculi (Figs. 9*a, b; see also* Ito, 1961, Helander, 1981, and Gibert & Hersey, 1982), which are absent in amphibia.

A preliminary glance at Table 1 (p. 26), to be discussed in more detail later, shows that, as a result of these four levels of folding, the actual area of apical or basolateral membrane exceeds the nominal smooth surface area by a factor of at least many hundreds, possibly thousands.

One obvious question posed by micrographs of resting oxyntic cells is whether there is any direct continuity between the stomach lumen and the intracellular network of smooth membranes. Four findings indicate that the answer is "no" for resting cells. First, in high power micrographs one

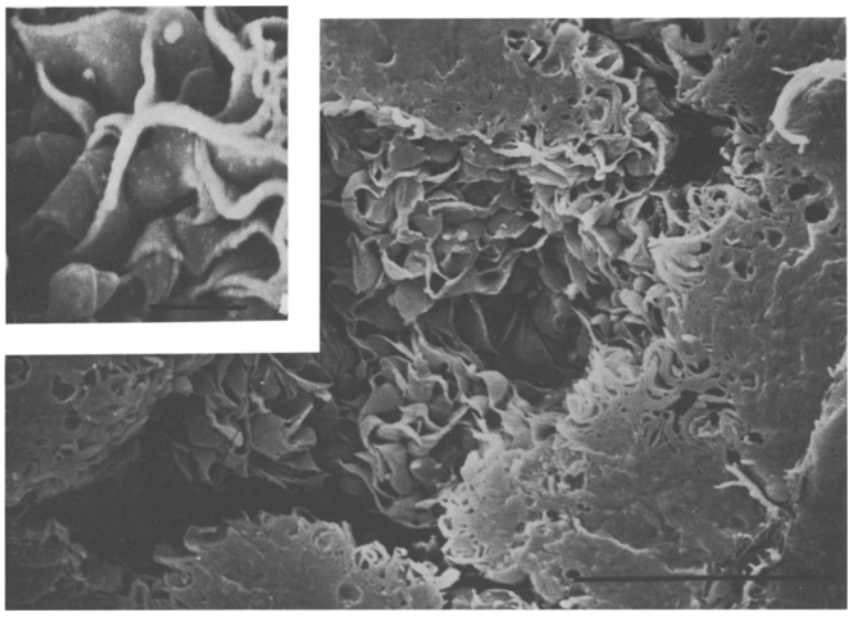

Fig. 8. SEM from the same mucosa as in Fig. 6. The surfaces of several oxyntic cells within a gastric gland have been exposed by cryofracture. Where the fracture face passes through the cell surface, it has the appearance of thin-sectioned material. The cell surfaces are covered with flattened sheets of membrane (lingulae). Bar = 10 μm. Inset shows higher magnification of surface (bar 2.5 μm). (From Logsdon and Machen, 1982*b*, reproduced from The Anatomical Record, published for the Wistar Press by Alan R. Liss, Inc.)

always observes a tubule-free zone of cytoplasm directly beneath the apical plasma membrane (Fig. 4). Second, and third, the macromolecular tracers peroxidase and microperoxidase do not penetrate into the tubular network in resting cells, though they do penetrate in stimulated cells (Sedar, 1969; Forte & Forte, 1970). Fourth, the intramembranous particle distribution (as determined by freeze fracture) differs markedly between the intracellular membrane and the apical membrane, suggesting that the particles cannot easily move between the two sets of membranes (Black, Forte & Forte, 1980*a*).

Histamine stimulation causes a dramatic change in the membrane ultrastructure of oxyntic cells. This change begins within about 3 min in the piglet gastric mucosa (Forte, Machen & Forte, 1975) and is complete within 30–45 min in both amphibian and mammalian cells. In isolated rabbit glands, where diffusion limitations are reduced, the change occurs even faster: membrane elaboration begins within 1 min of histamine stimulation and is essentially complete within 5 min (Gibert & Hersey, 1982). This study of isolated glands confirmed that ultrastructural changes precede the onset of acid secretion by many minutes, as in the intact mucosa (Forte et al., 1977). This result parallels the finding that electrical changes similarly precede the onset of acid secretion (Fig. 2).

The most obvious change in structure with histamine stimulation is the appearance of what appear to be long, slender, and sometimes branched microvilli at the apical surface (Fig. 9*a*). In the mammal, transmission (Fig. 9*b*), freeze fracture (Leeson, 1972; Ito & Schofield, 1974), and scanning (Osawa & Ogata, 1978) electron microscopic studies have all confirmed that these membrane projections are, indeed, microvilli. In lower vertebrates, though, freeze fracture (Forte & Forte, 1971) and scanning (Fig. 4; elasmobranchs, Rebolledo & Vial, 1979; frogs, Logsdon & Machen, 1982*b*; birds, Vial et al., 1979) electron microscopy has shown that the projections are actually flattened sheets of membrane, termed lingulae or microplicae.

With the increase in apical membrane area on histamine stimulation goes a decrease in smooth intracellular membrane (Figs. 7*b* and 9*b* and Table 1). Hence it is now generally accepted that acid secretion involves an interconversion of these two types of membrane, but the transition has been difficult to study, and its mechanism remains controversial. Two types of mechanisms have been proposed, which have been reviewed recently (Forte et al., 1982; *see also* Gibert & Hersey, 1982) and which we summarize more briefly. One hypothesis is fusion between apical membrane and the intracellular tubules (Forte, Machen & Forte, 1977; Forte et al., 1982). Alternatively, an osmotic swelling hypothesis does not require membrane fusion but postulates that the tubules and the apical membrane are joined at all times (Berglindh et al., 1980*b*). On this interpretation the tubules would be in a super-collapsed form in the resting state but would be opened by the water transport accompanying acid secretion, thereby exposing the previously collapsed microvilli.

It has been difficult to obtain conclusive proof

of membrane fusion during histamine stimulation, nor would one expect conventional electron microscopic techniques to stand much chance of "catching" a rapid fusion event if it occurred. Rapid freezing techniques could offer a more sensitive test of the fusion hypothesis. However, four lines of evidence argue that osmotic swelling alone does not explain conversion of tubular membrane into apical membrane:

(a) As mentioned above, four findings, such as nonpenetration of macromolecular tracers, indicate no free communication between the intracellular tubules and the stomach lumen in the resting state.

(b) Simple expansion of a collapsed space would not transform the tubular structures of resting cells into the flattened membrane sheets of stimulated cells in elasmobranchs, frogs, and birds without some drastic change in membrane geometry.

(c) There are several reversible experimental maneuvers that abolish acid (and presumably water) secretion, such as SCN^- (Hersey et al., 1981) and Na^+-free or K^+-free solutions (Logsdon & Machen, 1982*a*). These maneuvers do cause apical lingulae to assume a collapsed state with membranes closely apposed (Fig. 10), as reasoned in the osmotic swelling hypothesis. However, this appearance clearly differs from the appearance of the resting cell (Figs. 3, 4). Further, when these collapsed cells are treated with the histamine H_2 antagonist cimetidine, they revert to a normal resting appearance with cytoplasmic tubules and short microvilli at the apical surface (Logsdon & Machen, 1982*a*).

(d) Finally, Gibert and Hersey (1982) have shown that the original experimental evidence for the osmotic swelling hypothesis (Berglindh et al., 1980*b*) was based on incorrect interpretation of micrographs. Treatment of resting rabbit glands with high K^+ concentrations plus 1 mM aminopyrine causes expansion of canalicular spaces, but not of the tubulovesicular spaces as Berglindh et al. assumed.

Present evidence now suggests that the ultrastructural transition involves membrane fusion as well as osmotically-driven hydrostatic expansion of closely apposed membrane. In frog gastric mucosa the fusion events may occur not only between tubules and the apical membrane but also among intracellular tubules themselves (Logsdon & Machen, 1982*b*), thereby forming the sheets of membranes observed in the scanning electron microscope (Fig. 8). Because there appears to be a role of transmembrane osmotic gradients in fusion events both in artificial membranes (Zimmerberg, Cohen & Finkelstein, 1980) and in toad bladder (Kachidorian, Muller & Finkelstein, 1981), a hyperosmotic tubule lumen (possibly provided by KCl movement from cell to lumen) may play two roles in the gastric mucosa: to allow membrane fusion, and then to cause expansion of collapsed microvilli and microplicae. Cytoplasmic structural and contractile elements, such as microtubules and microfilaments, may also be involved.

Morphometric analysis of micrographs of resting and stimulated oxyntic cells has confirmed that there is an interconversion between the cytoplasmic tubular structures and the apical membranes. Thus, as shown in Table 1, during stimulation of frog or dog oxyntic cells there is a 2.5-fold decrease in tubular membrane while there is a seven- to 10-fold increase in apical membrane area (*see also* Schofield, Ito & Bolender, 1979; Gibert & Hersey, 1982). For two reasons, however, the actual values for membrane area need to be viewed with caution, and the data of Table 1 do not suffice to test whether there is conservation of total membrane. First, preparation of tissues for electron microscopy usually causes shrinkage. Second, in stimulated tissues some membrane that appears to be located intracellularly "beneath" the apical surface may actually be part of the apical membrane exposed to the stomach lumen. Thus, morphometric analysis necessarily underestimates the area of exposed apical membrane of these stimulated cells. Quantitation of actual area is a problem for which we think that impedance analysis may be especially helpful, as we shall discuss.

In contrast to these large changes in apical membrane area with stimulation, basolateral membrane area exhibits no major change with stimulation (Table 1, and Schofield et al., 1979).

Finally, we mention that fusion of cytoplasmic vesicles or tubules with apical or basolateral membranes may prove to be a common way of controlling ion transport in epithelia, though the extent of vesicular fusion is much smaller in other reported epithelial examples than in gastric mucosa. Recently investigated examples include the following. (1) Antidiuretic hormone stimulates fusion of cytoplasmic vesicles containing water permeation "channels" with the apical membrane of toad bladder cells (Gronowicz, Mazur & Holtzman, 1980; Muller, Kachidorian & Discala, 1980; Wade, Stetson & Lewis, 1981). In this case, the apical membrane area appears to increase by about 33% (Wade et al., 1981). (2) Stretch-induced fusion of vesicles with the apical membrane can cause up to a 20% increase of apical area in rabbit

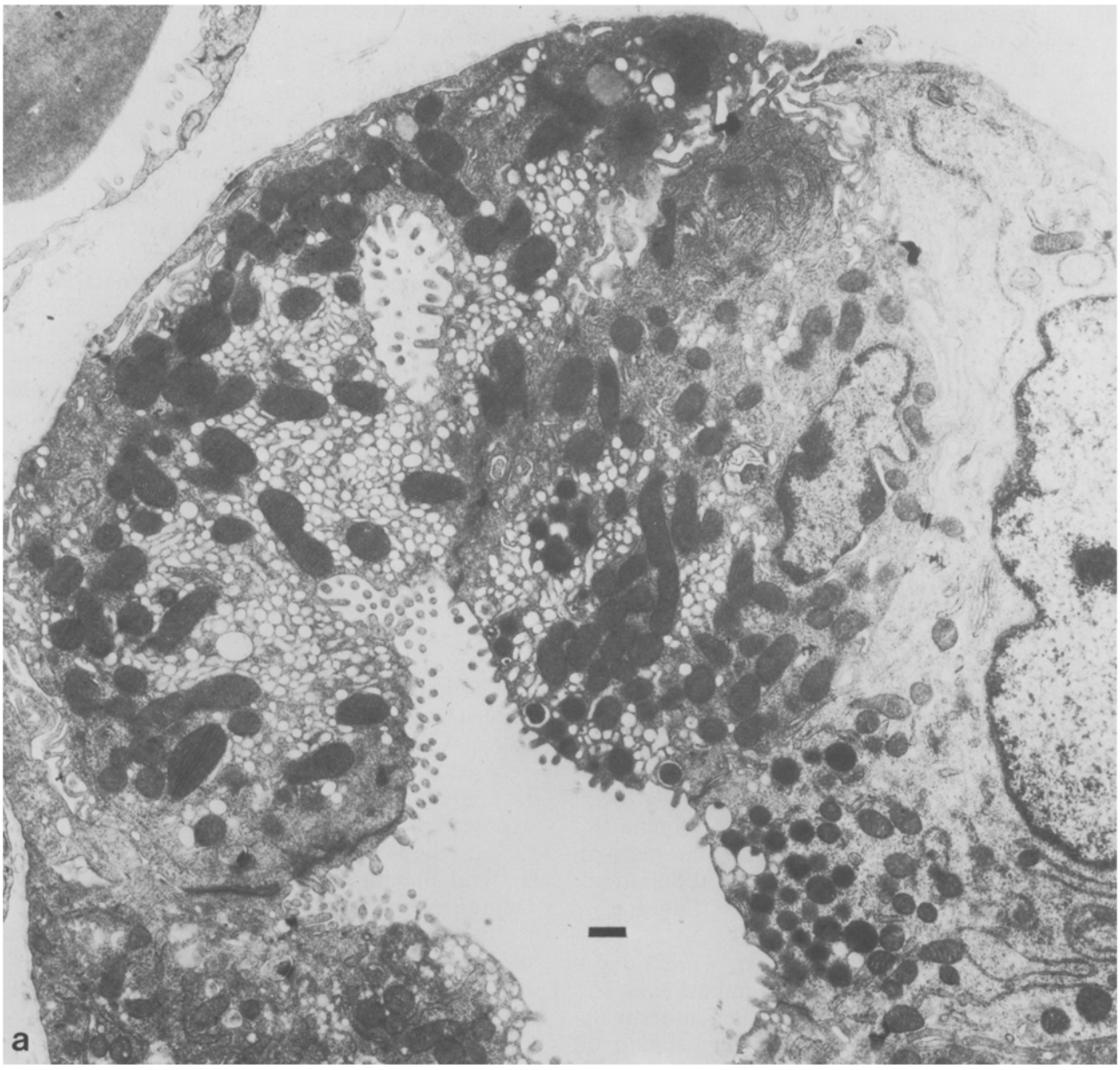

Fig. 9. TEM micrographs of oxyntic cells from resting and secreting gastric mucosa of piglet. Bars = 1 μm. (a) Resting mucosa. Two oxyntic cells are shown bordering the lumen of a gastric gland. Note the intracellular canaliculus, absent from frog gastric mucosa and making contact with the lumen in another plane of the section. Luminal and canalicular surfaces are studded with short stubby microvilli, many of which are cut in cross-section and appear as detached circles. Tubulovesicles within the cell also appear in cross-section. The folded nature of the basolateral membrane of these mammalian cells appears as basal infoldings and as folds of lateral membrane within the intercellular spaces.

urinary bladder (Lewis & de Moura, 1982). This increase in area by fusion may be important in permitting the bladder to accommodate large variations in urine content and degree of stretch. (3) In turtle bladder active H^+ pump sites are inserted into the apical membrane by fusion of cytoplasmic tubules and vesicles with the apical membrane (Gluck, Cannon & Al-Awqati, 1982). The apical membrane is folded into small microplicae (Stetson & Steinmetz, 1982) similar to those of the frog oxyntic cell (Fig. 10). (4) Increases in Na^+ transport in frog skin have been associated with increased numbers of cytoplasmic vesicles or vacuoles (Voute, Möllgard & Ussing, 1975).

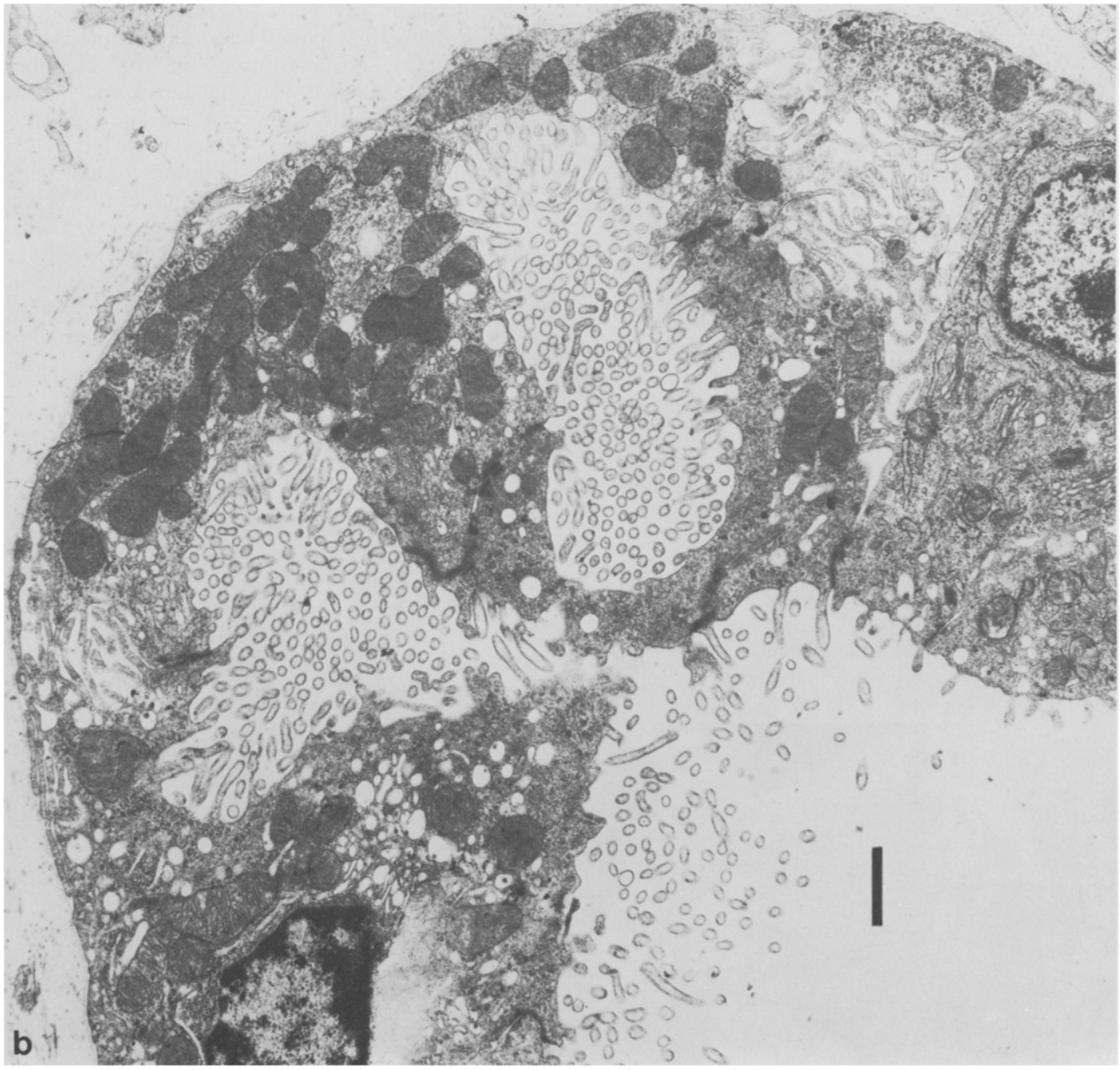

Fig. 9. (*b*): Maximally stimulated piece of mucosa from the same tissue as the resting piece seen in Fig. 9*a*. Few tubulovesicles remain in comparison with the resting mucosa. Instead, the canalicular and apical surfaces are covered with microvilli, most of which are seen in cross-section

Permeability and Conductances of the Junctions, Apical Membrane, and Basolateral Membrane

Like small intestine and gallbladder, the stomach transports large volumes of nearly isotonic fluid (*see* Durbin & Helander, 1978). In the stimulated state the stomach's transepithelial resistance is as low as that of small intestine and gallbladder, two examples of "leaky epithelia" in which ion conductance is known to be largely paracellular (via the junctions). If this were all we knew about gastric mucosa, we would take it too for a leaky epithelium, and we would be puzzled how it can maintain a 10^6:1 gradient of H^+ in the face of such junctional leakiness. Yet in other respects, such as

Table 1. Stereological data on oxyntic cell membranes

Species	Membrane	Surface density S_V (m^2/cm^3)		Cell surface area (cm^2/cm^2 of flat surface)	
		Resting	Stimulated	Resting	Stimulated
Dog	Apical	0.21[a]	2.27[a]	53[a]	568[a]
	Cytoplasmic tubules	6.05[a]	2.38[a]	1513[a]	595[a]
	Basolateral	0.91[a]	0.96[a]	228[a]	240[a]
Frog	Apical	0.15[b]	1.09[b]	–	188[a]
	Basolateral	–	0.95[a]	–	89[a]

For studies on dog oxyntic cells, "resting" refers to biopsies taken from stomachs of fasted, *in vivo* animals, while "stimulated" refers to biopsies taken from *in vivo* animals which had been stimulated intravenously with histamine. The numbers are two alternative indicators of membrane proliferation, expressed either as surface density (area of membrane per volume of tissue) or else as cell surface area (area of membrane per area of chamber). For studies on frog oxyntic cells, gastric mucosas were mounted for *in vitro* study and treated with 10^{-4} M cimetidine to obtain the resting condition or treated with 10^{-4} M histamine to obtain the stimulated state.

[a] Data taken from Helander et al., 1972.
[b] Data taken from Logsdon and Machen, 1982*b*.

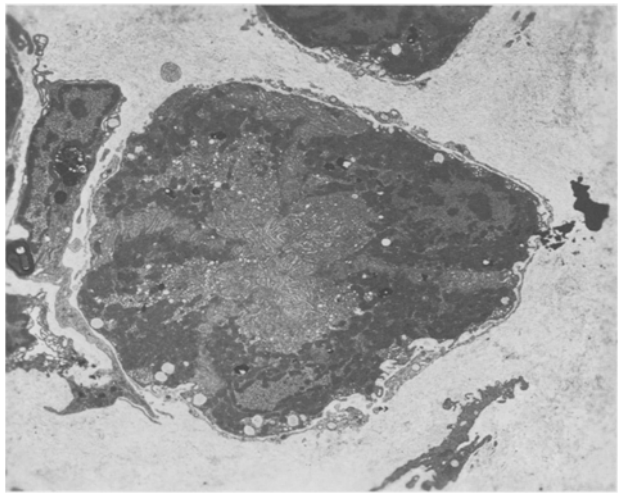

Fig. 10. Cross-section of a frog gastric gland that was first treated with histamine, dbcAMP, and IBMX to stimulate secretion, then with Na^+-free (choline replacement) solutions to inhibit secretion. Note that the apical lingulae are collapsed on each other (*compare* Fig. 3), presumably because HCl and water secretion is no longer occurring to cause membrane elaboration. ×1900

the large open-circuit voltage associated with active transport, the stomach resembles a tight epithelium. A possible explanation of this paradox is that junctions in the stomach are tight to H^+ and other ions, and that the low transepithelial resistance is merely a result of the enormous membrane folding that packs hundreds or thousands of cm^2 of membrane into 1 cm^2 of chamber opening. It remained for impedance analysis to confirm this interpretation by a quantitative test.

Apart from impedance studies, there have been two other attempts to quantitate junctional tightness in stomach. Microelectrode studies of *Necturus* gastric mucosa (Spenney, Shoemaker & Sachs, 1974) yielded the estimate that the paracellular pathway contributes only 21% of total transepithelial conductance. ^{22}Na back-flux measurements indicate a contribution of 25% in resting mammalian stomach (Machen, Silen & Forte, 1978; Tripathi & Rangachari, 1980) and even less in stimulated stomach (Machen et al., 1978). Both assessments rest on uncertain assumptions. The microelectrode measurements assume good electrical coupling between surface cells and oxyntic cells.[3] Coupling has been demonstrated among surface cells (Spenney et al., 1974) and among gland cells (Blum et al., 1971), but recent experiments argue against coupling between chief cells and oxyntic cells in isolated rabbit gastric glands (Hersey, Miller & May, 1982). The Na^+ back-flux experiments suffer from the possibility that the shunt might be anion selective.

Accepting the conclusion from these two assessments and from impedance studies that gastric junctional conductance is low, one can obtain qualitative information about the permeability properties of the apical and basolateral membranes. The method is to manipulate bathing solution composition while monitoring transepithelial PD and resistance. The resulting conclusions about apical or basolateral membrane properties apply to the whole stomach – i.e., are averaged over all cell types weighted by their conductance.

Experiments of this type have shown that the apical membrane of both resting and secreting stomach has significant conductance to Cl^- but very little conductance to K^+, H^+, or HCO_3^- (*see* Machen & Forte, 1979). The apical membrane has low G_{Na} in amphibia (Hogben, 1955), but in

[3] For clarity let us explicitly distinguish the two types of junctional pathways. The paracellular pathway permits (or fails to permit) ions and perhaps other very small molecules to pass between the luminal and serosal solutions, via the tight junctions and lateral spaces. This pathway has a high conductance in leaky epithelia and a low conductance in tight epithelia (Frömter & Diamond, 1972). The cell-to-cell pathway, alias electrical coupling, permits (or fails to permit) ions and other molecules of up to medium molecular weight to pass between adjacent cells, via specialized channels in the gap junctions (Loewenstein, 1981). Except in the paragraph to which this footnote applies, our discussion of the junctions through this review applies to the former pathway.

mammals (Machen et al., 1978) and reptiles (Hansen et al., 1975) it has a Na^+ conductance resembling the apical Na^+ channel of other tight epithelia like frog skin, toad bladder, and rabbit urinary bladder. Changes in transepithelial diffusion potentials in response to changes in (Cl^-) of the mucosal bathing solution imply high G_{Cl} of the apical membrane, and this is confirmed by accompanying changes in transepithelial conductance in piglet (Forte & Machen, 1975) and frog (Manning & Machen, 1983) gastric mucosa.

At the basolateral membrane it was shown some time ago that conductance is mainly to K^+ and Cl^- ($G_K/G_{Cl} \sim 3$), with negligible conductance to H^+ and HCO_3^- (Harris & Edelman, 1964; Spangler & Rehm, 1968). Thus, changing (K^+) and (Cl^-) of the serosal solution at constant product causes transepithelial PD to change with a 50–60 mV slope (Harris & Edelman, 1964), with most of this change arising from the basolateral membrane (Spenney et al., 1974). However, recent experiments indicate that the conductance properties of the basolateral membrane are more complex than originally thought. Thus, in both resting and secreting tissues, changing (Na^+) of the serosal solution changes the transepithelial PD in the direction expected if it were (Cl^-) of this solution that were being altered (Machen & McLennan, 1980; Carrasquer et al., 1982)! A similar effect is observed when the (HCO_3^-) of the serosal solution is altered in resting tissues (Manning & Machen, 1982; Takeuchi & Silen, 1982). It has also been found in resting tissues that, with Na^+-free or HCO_3^--free serosal solutions, changing (Cl^-) of the serosal solution has no effect on the PD (Takeuchi & Silen, 1982; Manning & Machen, 1983)! In Cl^--free solutions changing (Na^+) or (HCO_3^-) has little effect on the PD (Takeuchi & Silen, 1982; Manning & Machen, 1983). Finally, Cl^--free or HCO_3^--free serosal solutions reduce the PD change in response to alterations of K^+ (Manning & Machen, 1983). These remarkable and unexpected results suggest important interactions among the conductance pathways for Na^+, K^+, Cl^-, and HCO_3^-, interactions that we shall consider further in the section "Models of Ion Transport."

It is generally agreed that the basolateral membrane contains not only these conductance pathways but also two exchange "carriers." One is a neutral Cl^-/HCO_3^- exchanger inferred for the oxyntic cells on the basis of electrophysiological experiments (Rehm & Sanders, 1975). The other is the usual active, electrogenic, ATP-driven Na^+/K^+ pump, inferred for all cells of the epithelium from studies of the effects of ouabain (Davenport, 1962; Forte & Machen, 1975; Carrasquer et al., 1981) and K^+ (Schwartz et al., 1981) on transport and voltage. These two exchangers are important in maintaining intracellular pH and in electrogenic Cl^- and HCO_3^- secretion (see below).

Studies of Apical Membranes Isolated from Oxyntic Cells

In recent years the ultrastructural and electrophysiological approaches just described have been supplemented by a valuable new biochemical approach: the isolation and study of apical membranes from resting oxyntic cells, as so-called gastric microsomes. These membrane vesicles orient with the normal "luminal face" inside and the normal "cytoplasmic face" outside. The earliest studies on these vesicles showed that they could accumulate H^+ (Lee, Simpson & Scholes, 1974) within the vesicular space. This H^+ transport depended on the presence of ATP and Mg^{++} outside and K^+ inside the vesicles. H^+ accumulation was stimulated by the addition of the K^+ ionophore valinomycin, presumably because it allowed K^+ easy access to the inside of the vesicles. Under these conditions the rate of H^+ accumulation depended on the magnitude of the Cl^- conductance in the vesicles (Lee et al., 1979). Surprisingly, the native conductance of gastric microsomes to Cl^- and K^+ was very low. Thus, $t_{1/2}$ for passive equilibration of K^+ or Cl^- between the vesicle contents and outside was $\sim 1/2$ hr (Schackmann et al., 1977), and the H^+ gradient dissipated only in the simultaneous presence of valinomycin and the protonophore FCCP. However, neutral K^+/K^+ exchange is very rapid and yields $t_{1/2} \sim 10$ sec. These observations suggest, and further experiments confirm, that the H^+ "pump" of gastric microsomes operates as a neutral, 1:1 H^+/K^+ exchanger (Sachs et al., 1976; Schackmann et al., 1977; Lee & Forte, 1978).

One obvious difference between H^+ transport in microsomes and in intact gastric mucosa is that microsomes require valinomycin in order to form maximal H^+ gradients (Lee et al., 1974, 1979; Sachs et al., 1976). That is, the K^+ site for the K^+/H^+-ATPase is located on the inside of the vesicles, but net K^+ uptake across microsomes from resting oxyntic cells is so low that the K^+/H^+ exchanger cannot operate unless valinomycin is used to provide K^+ with artificial access to the inside of the vesicles. It was therefore an important step towards reconstituting a more realistic H^+-transporting system when Wolosin and Forte (1981)

found that vesicles prepared from stomachs previously stimulated to secrete H^+ exhibited maximal H^+ accumulation when K^+ was simply added to the external medium in the absence of valinomycin. It has now become clear that these so-called stimulation-associated (SA) vesicles contain, in addition to the K^+/H^+ exchanger, a neutral K^+/Cl^- cotransport system (symporter) that allows K^+ rapid access to the inside of the vesicle and thereby obviates the valinomycin requirement. The separate K^+ and Cl^- conductances of the SA vesicles as of gastric microsomes are low compared to the rates of K^+/Cl^- cotransport and K^+/H^+ exchange. However, both K^+/K^+ exchange and Cl^-/Cl^- exchange in SA vesicles are rapid, with $t_{1/2} \sim 10$ sec (J.M. Wolosin & J.G. Forte, *personal communication*). Sachs et al. (1982) have recently suggested that regulation of net KCl flux into the secretory lumen of the stomach depends on the activation of a Cl^- pathway to accompany the K^+ exchange pathway which appears always to be present in the membranes.

Thus, work on isolated vesicles has yielded much information about apical membrane permeability in resting and stimulated oxyntic cells. Nevertheless, numerous mysteries remain. Why is the K^+/Cl^- symport present in SA vesicles but not in gastric microsomes? That is, what regulates the symport? Why is Cl^- conductance high in intact gastric mucosa but low in both SA vesicles and microsomes? Is Cl^- conductance somehow "lost" during the isolation procedures? Is Cl^- conductance confined to the surface cells? Can the K^+/Cl^- symport ever operate in a conductive fashion that might manifest itself as Cl^- conductance in the intact mucosa?

We have referred to the H^+ accumulation mechanism of vesicles as a K^+/H^+ exchanger. More specifically, it is a H^+/K^+-activated ATPase: recent studies have not only clarified permeability properties of apical membrane but also identified ATP as the immediate energy source for H^+ transport and thereby resolved what had been a long-standing debate. Although most ion pumps run directly off of ATP, a redox mechanism has been entertained as an alternative explanation for gastric H^+ secretion. This question of the energy requirement for H^+ secretion has now been studied both in vesicles and in rabbit gastric glands. Initial measurements yielded values between 3 and 4 for the ratio of H^+ ions pumped to ATP molecules split (Sachs et al., 1976; Schackmann et al., 1977). As this value is higher than that expected if the energy for transport came only from ATP hydrolysis, elaborate transport schemes involving combinations of redox and ATPase mechanisms were proposed (Rabon et al., 1977; Sachs, Spenney & Lewing, 1978).

However, several findings indicate that redox components are probably not directly involved in H^+ transport across oxyntic cell apical membrane. For example, only cytochrome b_5, and no other cytochrome, has been found associated with the gastric mucosal apical membrane (Forte, Forte & Saltman, 1967; Lewin et al., 1977). Since cytochrome b_5 requires an electron acceptor such as cytochrome c to operate effectively, this membrane-associated b_5 probably represents contamination from smooth endoplasmic reticulum (J.G. Forte, *personal communication*). Direct evidence implicating ATP as a major source of energy for H^+ accumulation comes from recent experiments on rabbit gastric glands "shocked" by capacitance discharge, which renders the basolateral membranes but apparently not the apical membranes permeable to molecules as large as ATP. Addition of ATP to these shocked glands, after treatment with CN^-, N_3^-, or amytal to inhibit the cytochromes completely, still resulted in H^+ accumulation (Berglindh et al., 1980*a*). Reenstra and Forte (1981) have recently calculated that the H^+/ATP ratio of gastric microsomes under various bathing solution conditions is very close to 1, while Sachs et al. now argue that the ratio is close to 2.

Thus, available data for the H^+ pump of oxyntic cells appear to be explained by a "simple," neutral, ATP-driven K^+/H^+ exchanger, but the exact H^+/ATP stochiometry remains a difficult, important, and unsolved problem (*see also* Sachs et al., 1982).

Models of Ion Transport

Figure 11 synthesizes the electrophysiological and biochemical findings into a model of ion transport by gastric mucosa. This figure may look complicated and it should be: no simple-looking model could be faithful to reality for an epithelium with two major cell types and four major transported ions. Let us begin with HCl secretion.

The mechanism of H^+ secretion and of the accompanying Cl^- secretion by the oxyntic cell has now been fairly well established. At the apical membrane it involves both the neutral H^+/K^+ exchanger found in gastric microsomes and SA vesicles and the K^+/Cl^- neutral symport observed in SA vesicles alone. To pick an arbitrary point in the cycle as the start, K^+ and Cl^- move rapidly from the oxyntic cell to the gastric pit lumen via

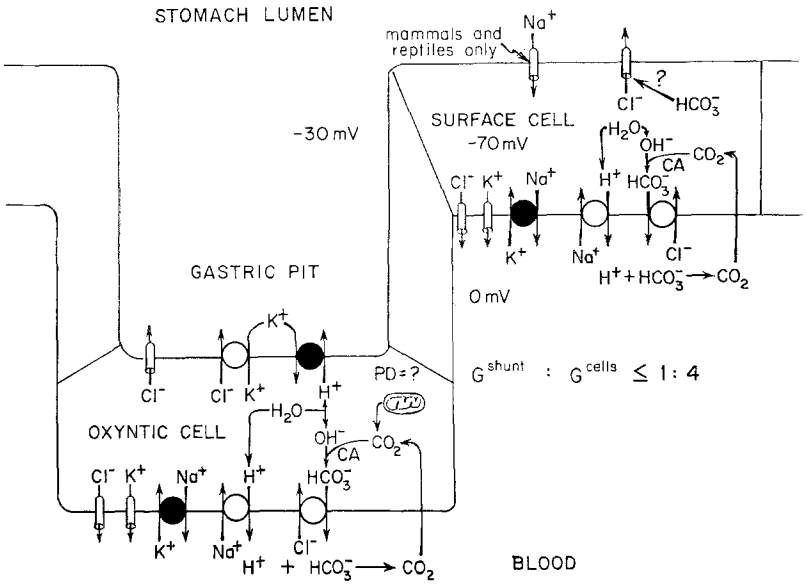

Fig. 11. Ion transport and conductance pathways in oxyntic cells and surface epithelial cells of gastric mucosa. Filled circles are active transport pumps driven by ATP. Open circles are cotransport or countertransport exchangers that do not consume energy. Long cylinders are conductance "channels," through which the predominant direction of net flux is shown by an arrow. *CA* = carbonic anhydrase. In the short-circuited state $I_{sc} = J^{Cl}_{net} - J^{H} + J^{Na}_{net}$. *See* text for discussion

the K^+/Cl^- symport. The K^+ is then immediately recycled back into the cell via the H^+/K^+-ATPase, in exchange for an H^+ that has been split from water. The net result is that the cell has secreted HCl. It remains unclear how K^+ exit via the K^+Cl^--symport can be coupled so tightly to K^+ uptake via the H^+/K^+ exchanger (Forte, Machen & Öbrink, 1980). A further puzzle is how to reconcile the electrogenicity of H^+ secretion by frog gastric mucosa in Cl^--containing solutions, and the neutrality of the H^+/K^+ exchanger.

The OH^- remaining in the oxyntic cell from the splitting of water is then neutralized by CO_2 in a carbonic-anhydrase-catalysed reaction to yield HCO_3^-, which then exits to the bloodstream across the basolateral membrane in neutral exchange for Cl^- (Rehm & Sanders, 1975; see also Forte and Machen, 1983). In addition to ridding the cell of the HCO_3^- left over from the reaction $CO_2 + H_2O \rightarrow H_2CO_3^-$ after secretion of H^+, the basolateral Cl^-/HCO_3^- exchanger also provides the Cl^- that will exit the apical membrane via the K^+/Cl^- symport to accompany the secreted H^+.

Gastric mucosa also secretes Cl^- in excess of H^+, generating a short-circuit current. This separate Cl^- transport is less well understood than is HCl transport, partly because it appears to operate both in the surface cells (Machen & Zeuthen, 1982) and oxyntic cells (McLennan, Machen & Zeuthen, 1980), perhaps by the same mechanism in the two cell types. Cl^- uptake across the basolateral membrane is uphill, while exit across the apical membrane is downhill. This follows from the intracellular voltage (-50 to -70 mV in short-circuited surface cells) and from direct measurements of intracellular (Cl^-) by ion-specific microelectrodes (Machen & Zeuthen, 1982). The same measurements further show that apical membrane permeability to Cl^- is high enough to account for the observed Cl^- exit, presumably through an anion conductance channel. Since there also appears to be a net outwards driving force for OH^- and HCO_3^- at the apical membrane, these ions may exit by the same channel, though at a lower rate than Cl^-. This channel may account for HCO_3^- secretion by surface cells (Flemström & Garner, 1982; Takeuchi & Silen, 1982).

At the basolateral membrane, uphill Cl^- uptake may involve the Na^+-dependent cotransport mechanism postulated for most Cl^- secretory systems (Frizzell, Field & Schultz, 1978; McLennan et al., 1981). In this model Cl^- uphill movement is coupled to Na^+ downhill movement. A further complication in resting gastric mucosa is that electrogenic Cl^- transport depends not only on Na^+ but also on (HCO_3^-) of the serosal solution (Schiessel et al., 1980; Manning & Machen, 1982). This suggests operation of the double-exchanger that appears to account for much of the neutral Na^+/Cl^- cotransport in proximal tubule (Aronson, 1981; Reenstra et al., 1981) and small intestine (Liedtke & Hopfer, 1982; *see also* Sachs et al., 1982). The double exchanger yields NaCl accumulation by combining a Cl^-/HCO_3^- exchanger with a Na^+/H^+ exchanger by which Na^+ enters the cell in exchange for H^+. The postulated alkalinization of the cell is supported by cell pH measurements with DMO (Ekblad, 1980; Manning & Machen, 1982) or with pH-sensitive dyes (Hersey, 1979), which show that resting cell pH

is 7.0–7.4, more alkaline than predicted for passive distribution of H^+ across the basolateral membrane. The resulting raised intracellular (HCO_3^-) may then drive Cl^- entry through the Cl^-/HCO_3^- exchanger, whose presence in the basolateral membrane of oxyntic cells had already been surmised by Rehm and Sanders (1975). Thus, the only new postulates of this model are that the same Cl^-/HCO_3^- exchanger occurs in surface cells; the presence of a parallel Na^+/H^+ exchanger in basolateral membranes is suggested by the study of Burnham and Sachs (1982). Note that this scheme involves CO_2 recycling across the basolateral membrane not only in oxyntic cells, as has long been assumed in connection with H^+ secretion, but also in surface cells. The Na^+ that enters cells across the basolateral membrane in exchange for H^+ by this scheme is recycled out across the same membrane by the Na^+/K^+ ATPase.

An interesting feature of this scheme not indicated in Fig. 11 is that it suggests interaction between the rate of *neutral* basolateral NaCl uptake, on the one hand, and the *conductances* of the apical membrane to Cl^- (G_{Cl}^m) and of the basolateral membrane to K^+ (G_K^s), on the other hand. By the Cl^- transport scheme of Fig. 11 I_{sc} in the short-circuited state would be carried by Cl^- across the apical membrane but by K^+ across the basolateral membrane. Obviously, the relations between basolateral NaCl transport, apical G_{Cl}, and basolateral G_K are critical to this scheme. Somehow, increases of neutral NaCl uptake need to be reflected in increases of G_{Cl}^m and G_k^s – e.g., as a result of both conductances being regulated by a cellular component that "senses" the rate of NaCl transport.

A similar problem arises in Na^+-transporting tight epithelia, where basolateral Na^+ transport somehow controls apical Na^+ conductance (Lewis, Eaton & Diamond, 1976) and basolateral K^+ conductance (Schultz, 1981). The former control involves negative feedback: decreased basolateral Na^+ extrusion tends to raise intracellular (Na^+), suppressing apical Na^+ conductance, perhaps through secondary changes in intracellular Ca^{++} produced by Na^+/Ca^{++} exchange dependent on cell Na^+ (Grinstein & Erlij, 1978; Taylor & Windhager, 1979; Chase & Al-Awqati, 1981; Taylor, 1981). The direction of the postulated feedback in gastric mucosa would be opposite to that in Na^+-transporting tight epithelia: increases in Na^+ (and Cl^-) entry would increase cell (Ca^{++}), as in the Na^+-transporting tight epithelia; but this increase in cell (Ca^{++}) would then *increase* G_{Cl}^m (as observed in colon: Frizzell, 1976) and also G_K^m (e.g., through a Gardos-like effect).

The postulated feedbacks probably explain the otherwise puzzling observation that changes in electrogenic Cl^- transport are associated with parallel changes in transepithelial conductance (Forte & Machen, 1983). For example, inhibition of Cl^- secretion by use of Cl^--free or HCO_3^--free solutions reduces apparent G_K^s and G_{Cl}^m. Similarly, the feedbacks plus the operation of the Na^+/H^+ and Cl^-/HCO_3^- exchangers may explain the bizarre interdependences of effects of serosal bathing Na^+, Cl^-, HCO_3^-, and K^+ on PD discussed on p. 27. Vesicle or microelectrode studies are needed for elucidation of these interesting problems.

Finally, Na^+ absorption by mammal and reptile stomach involves Na^+ entering the surface cells across the apical membrane by an amiloride-sensitive channel and leaving across the basolateral membrane by the Na^+/K^+ ATP-ase (Machen et al., 1978; Machen & Forte, 1979; Tripathi & Rangachari, 1980). This mechanism appears very similar to the Na^+ transport mechanism of other tight epithelia such as frog skin (Helman & Fisher, 1977), amphibian urinary bladder (Higgins et al., 1975), and rabbit urinary bladder (Lewis & Diamond, 1976), with the exception that the possibility of stimulation by aldosterone has not yet been carefully examined for Na^+ absorption by the stomach.

With this review of gastric electrophysiology, ultrastructure, and biochemistry as a background, we now turn to impedance analysis in an attempt to integrate some of the findings just described.

Impedance Analysis of Epithelia

Why Use Impedance Analysis to Study Epithelia?

The attraction of electrophysiological methods for measuring ion permeabilities lies in their rapidity and accuracy compared to tracer methods. In model membranes and single cells of simple geometry such as erythrocyte, nerve, and flat lipid bilayers, it is in principle straightforward to extract membrane conductance per unit area from steady-state DC resistance measurements. In epithelia this extraction is no longer straightforward, because transepithelially measured conductance must be resolved into its dependence on at least three structures: the apical cell membrane, basolateral cell membrane, and paracellular shunt (junctions plus lateral spaces).

For selected epithelia this resolution has been accomplished by either or both of two methods: cable analysis (e.g., Frömter & Diamond, 1972;

Spenney et al., 1974; Reuss & Finn, 1975); and measurement of voltage-divider ratio and transepithelial resistance while carrying out a procedure expected to change only one of the three resistors, such as alteration of apical membrane resistance with amiloride or nystatin (e.g., Reuss & Finn, 1974; Frömter & Gebler, 1977; Lewis, Eaton, Clausen & Diamond, 1977). Each method has disadvantages. Cable analysis is technically difficult and time-consuming because it requires two intracellular microelectrodes and puncturing many cells; the data can be difficult to fit, and can be hard to interpret if the epithelium is not in the form of a flat sheet (Zeuthen, 1980). The resistor-variation method requires finding such a method for the epithelium of interest, making measurements rapidly enough that other resistors do not also change, and proving that this condition is satisfied.

Thus, one use of impedance analysis in epithelia is as an alternative procedure to separate the components of transepithelial resistance by means of equivalent circuit analysis. In addition, impedance analysis can do two things that cable analysis and the resistor-variation method cannot: measuring membrane areas, and measuring membrane configuration.

Membrane Area. A glance at Figs. 3–10 will remind one of the need for a good method to measure membrane areas. A chamber area of 1 cm^2 corresponds to some unknown larger membrane area of gastric mucosa, because of folding at many levels: the whole surface has gross folds, it is further infolded into gastric pits and glands, the basolateral membrane is irregular and expanded by the lateral spaces, and the apical membrane is vastly expanded by microvilli and tubules. To what should one normalize membrane measurements such as conductance or current? If one merely normalizes to chamber area or tissue weight, one is ignoring the fact that apical and basolateral membrane areas of the same epithelium may differ by an order of magnitude, and that areas of the corresponding membrane may differ by several orders of magnitude between different epithelia. As one example, gastric mucosa may have a lower transepithelial resistance than intestine or gallbladder mounted in the same chamber: is this because gastric mucosa has leaky junctions like gallbladder, or because it has tight junctions but hundreds of m^2 of chamber area? As another example, the resistance of gastric mucosa apparently drops with onset of acid secretion: is this due to an increase in conductance per unit membrane area, or to an increase in membrane area per unit chamber area?

The best solution to the problem of measuring true membrane area is to measure membrane capacitance. Capacitances of diverse biological membranes cluster between 0.8 and 1.2 $\mu F/cm^2$ (Davson, 1964; Cole, 1972). Hence a membrane capacitance of 1 μF indicates a true membrane area of approximately 1 cm^2. Impedance analysis yields both capacitance and resistance, whereas cable analysis and the resistor-variation method yield resistance alone.

Membrane Configuration. Cable analysis and the resistor-variation method yield no information about membrane configuration. Impedance analysis does, because the impedance of a folded membrane that behaves as a distributed resistor varies with current frequency. From the frequency dependence one can calculate the ratio of cross-sectional area to length for the membrane fold in the living state, without the fixation artifacts and morphometric problems introduced by electron microscopy. Examples of such folds are the gastric glands, apical microvilli, apical tubules, and lateral intercellular spaces of gastric mucosa.

Thus, specific goals of impedance analysis for gastric mucosa would include: resolution of apical, basolateral, and junctional resistances; estimates of apical and basolateral membrane areas and configurations, and how they change with acid secretion; understanding of why mucosal resistance changes with acid secretion; and an answer to the paradox why gastric mucosa appears to have a low resistance, yet otherwise has the hallmarks of a tight epithelium.

Theory and Practice of Impedance Analysis

Impedance is the ratio of measured transmembrane voltage to applied current when one applies a constant sinusoidal current across a membrane. Impedance varies with frequency of the applied current. Two quantities are measured at each frequency: the ratio (in ohms) of the magnitudes of the voltage and the current; and the phase angle (in degrees) by which the applied sinusoidal current leads the resulting sinusoidal voltage.

Ideally, impedance analysis would proceed in four steps:

First, measure impedance over a wide range of frequencies, sufficiently rapidly that membrane parameters remain constant over the required measuring time.

Second, plot or represent the data in a way that is sensitive to effects of membrane parameters.

For example, if one wants the value of a membrane parameter that affects impedance mainly at high frequency, the representation of the data should not compress high-frequency data at the expense of low-frequency data.

Third, formulate a morphologically based electrical equivalent circuit, whose model parameters correspond to resistances, capacitances, and configurations of actual structures.

Finally, fit the model to the data, extract values of model parameters, validate these values by independent measurements in order to gain trust in the procedure, and go on to use the procedure to answer unsolved questions.

We now discuss four classes of difficulties in the execution of this idealized procedure.

Method of Gathering Data. The most direct approach to impedance analysis is to apply a sinusoidal current of one frequency and measure impedance, repeat the measurement at another frequency, and proceed in this way to cover the desired range of frequencies, periodically remeasuring impedance at some standard frequency to check that the preparation is remaining in a steady state.

The drawback to this procedure is that it is time-consuming. At each frequency one should wait at least a dozen cycles to check that the voltage sinusoids reach their final form. An impedance run that covers six frequencies per frequency decade from 1 to 10,000 Hz requires on the order of 10 min. This limits use of impedance analysis to study of maintained steady states and precludes the study of interesting rapid phenomena, such as resistance changes in gastric mucosa with onset of acid secretion.

An alternative procedure introduced by Teorell (1946) is "square wave analysis" or "transient analysis": measuring the voltage response to a square current pulse. By Fourier analysis the current pulse and voltage response can each be converted to a sum of sinusoids. Thus, transient analysis is in principle similar to measuring the response to each current frequency separately. The virtue of transient analysis is that in effect all frequencies are measured simultaneously rather than sequentially, so that data gathering is very rapid (<1 sec for the usual impedance run).

Unfortunately, transient analysis suffers from two disadvantages whose seriousness has been appreciated only recently. First, in a circuit of linear *RC* elements a square current pulse yields a voltage response consisting of a sum of exponentials, whose amplitudes and time constants must be determined by curve fitting. If there are two or more time constants not widely separated from each other, the accurate determination of these time constants is difficult and sometimes impossible, as applied mathematicians have stressed (Lanczos, 1956; Acton, 1970) and biologists tend to ignore. Second, although it might at first seem that resolution of a square wave into simultaneous frequencies offers the same information content as sequentially measured frequencies, this is not true. Yes, a square wave does consist of a sum of frequencies. But the frequency spectrum of a square wave is such that amplitude decreases hyperbolically with frequency. Thus, transient analysis overweights low frequencies, whereas measuring frequencies sequentially weights them equally. This is a fatal drawback of transient analysis in epithelia, as effects of distributed resistors appear at middle to high frequencies. For example, Clausen, Lewis and Diamond (1979, their Figs. 2 and 3) showed that if one varies the area/length parameter of the distributed resistor over a reasonable range in a model circuit corresponding to rabbit urinary bladder, the resulting voltage responses to a square wave are indistinguishable, whereas curves of phase angle as a function of frequency are readily distinguishable.

One thus arrives at a dilemma. Sequential measurement of frequencies is adequate for studying a stable preparation but too slow to study a rapid process. Transient analysis is rapid, but extraction of parameters is sometimes not possible, and the method is insensitive to middle- and high-frequency effects. The resolution of this dilemma may come from methods under development that in effect simultaneously apply many frequencies but with the desired weighting. Examples of such wave forms include burst sine waves (Warncke & Lindemann, 1979), pseudo-random Gaussian noise (Mathias, Rae & Eisenberg, 1979), and pseudo-random binary noise (Clausen & Fernandez, 1981).

Use of Morphologically based Models. The goal of impedance analysis in biological systems is to learn something about individual membranes. It follows that the equivalent electrical circuit used to fit the data must be morphologically realistic, so that extracted values of model parameters may correspond to resistances and capacitances of actual membranes. A good example of the stages in development of increasingly realistic models is provided by the history of equivalent circuit analysis in frog skeletal muscle (Valdiosera, Clausen & Eisenberg, 1974; Mathias, Eisenberg & Valdiosera, 1977).

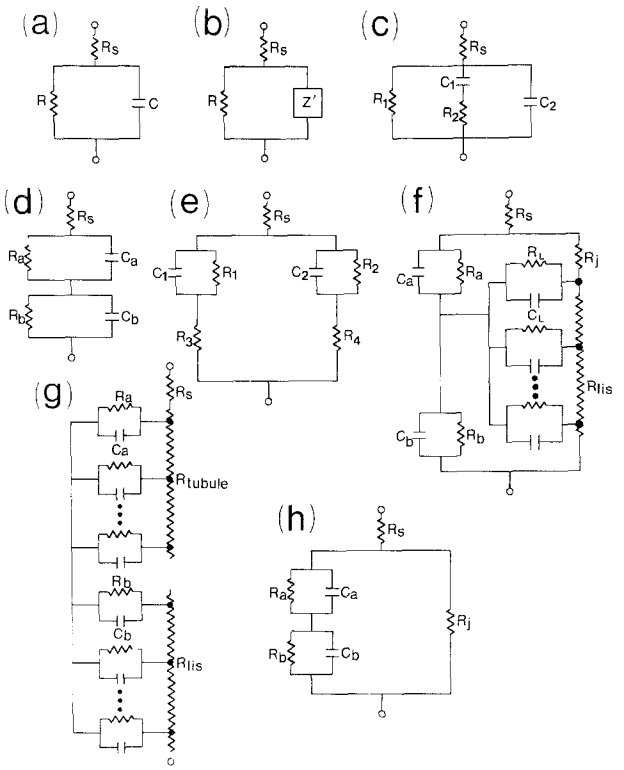

Fig. 12. Eight different circuit models that have been used to analyze impedance data for epithelia. *See* text for discussion

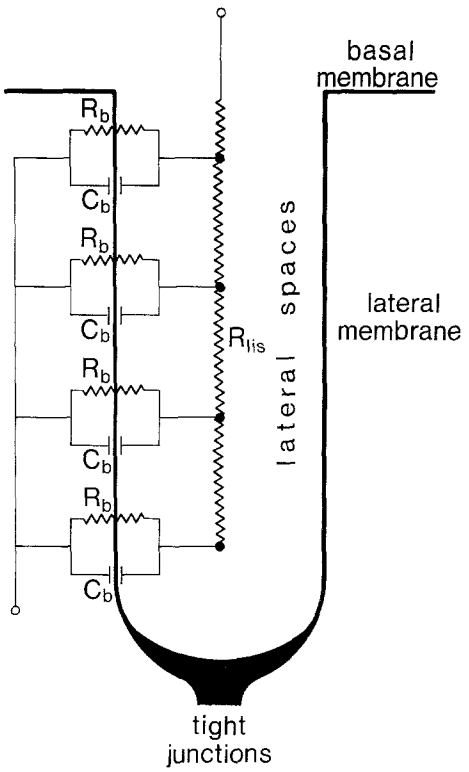

Fig. 13. Representation of the lateral intercellular spaces as a distributed resistor. R_{lis} is the longitudinal resistance to current flow along the lateral intercellular spaces, proportional to their solution resistivity, length, and reciprocal of their cross-sectional area. The basolateral membrane is modelled as a series of *RC* subcircuits in series with a fraction of R_{lis} that depends on their position along the spaces. Membrane elements near the tight junctions are in series with the full value of R_{lis}; elements on the basal membrane, with none of it

Figure 12 illustrates the sequence of models used to date with variants and in combination, to fit epithelial impedance data. All these models use a series resistor to represent the extracellular and intracellular fluid, plus other elements to represent the membranes. The single *RC* subcircuit of Fig. 12*a* (Teorell & Wersäll, 1945) fails in realism because epithelia consist of two cell membranes in series. Misfits of data to this model were first treated by modelling the capacitor as a non-ideal capacitor (Fig. 12*b*; Brown & Kastella, 1965), or by inserting a series resistor-plus-capacitor subcircuit in parallel (Fig. 12*c*; Flemström, 1971). Both of these modifications were purely formal ones to accommodate the data without corresponding to actual biological structures. More realistic modifications were the use of two *RC* subcircuits in series, hopefully to correspond to the apical and basolateral membranes in series (Fig. 12*d*; Noyes & Rehm, 1970; Smith, 1971; Wright, 1974; also the slightly more complex Fig. 12*e*; Rehm & Tarvin, 1978); the addition of one (Fig. 12*f*) or two (Fig. 12*g*) distributed resistors, to correspond to lateral intercellular spaces (Frömter, 1972; Clausen et al., 1979), gastric pits (Ring & Sandblom, 1980), intestinal crypts (Clausen & Wills, 1981), or apical tubulovesicles (Clausen, Machen & Diamond, 1982); and the addition of a parallel resistor, to correspond to leaky junctions (Fig. 12*h*: Frömter et al., 1981; Clausen & Wills, 1981).

The presence of multiple cell types introduces complications into interpreting electrical measurements, or indeed any transport measurements, in epithelia. For example, if the parietal cells and surface epithelial cells of gastric mucosa have comparable impedance, *R* and *C* values extracted from the fit of impedance data to a model such as that of Fig. 12*d–h* do not have a simple biological interpretation but are complicated functions of the *R* and *C* values of more than one membrane (Rehm et al., 1976; Rehm & Tarvin, 1978).

The use of distributed resistors in epithelial models requires comment. Take the basolateral membrane of rabbit urinary bladder as an example (Fig. 13). This membrane is deeply infolded about the long and narrow lateral intercellular spaces (LIS), which are open at the basal end but electri-

cally closed by tight junctions at the apical end. Taking the length of the LIS as ca. 20 μm and their width as ca. 100 Å, solution resistivity of the experimental solution as 64 Ω-cm at 37 °C, and the epithelial cells as cubes 20 μm on a side, one calculates a longitudinal resistance to current flow along the LIS as 130 Ω-cm^2, related to chamber area (Clausen et al., 1979). The resistance of the basolateral membrane is about ten times higher. Hence at low current frequencies, where basolateral membrane current is determined largely by membrane resistance, one can neglect the resistance of the LIS. However, at high current frequencies membrane current becomes largely capacitative, and membrane impedance drops below the resistance of the LIS. Under these circumstances the LIS become important as a distributed resistor. That is, they constitute a resistance in series with the lateral membrane, but the series resistance varies with position along the membrane, being maximal at the end near the tight junctions and decreasing to zero at the open end (Fig. 13).

This reasoning is similar to that used in recognizing the role of the transverse tubular system in skeletal muscle as a distributed resistor. More generally, distributed effects may become important wherever one finds a long, narrow, fluid-filled, membrane-bounded space whose longitudinal resistance to current flow becomes comparable to membrane impedance at high frequencies. Structures of this form are encountered at several levels in epithelia. For instance, at the apical surface of gastric mucosa one encounters distributed resistors on at least three scales: the gastric pits at the grossest level, the apical membrane tubules at a finer level, and the microvilli and the spaces between them at the finest level. Since distributed effects increase with increasing frequency, transient analysis, which weights low frequencies, is ill equipped to detect distributed effects.

Distributed effects become partiticularly troublesome in leaky epithelia under experimental conditions where the LIS are collapsed. For example, earlier measurements of the resistances of the apical and basolateral membranes of the *Necturus* gallbladder (Frömter, 1972; Reuss & Finn, 1975) appear to have been overestimates by factors of 5 and 23, respectively, because of distributed effects (Frömter et al., 1981)! The tissues used in the earlier measurements were incubated in inadequately oxygenated solutions with low HCO_3^- concentration, conditions which reduce fluid transport, collapse the LIS, and make distributed effects more severe. Because R_b was initially estimated to be so large, Reuss and colleagues were forced to conclude that both K^+ (Reuss, Weinman & Grady, 1980) and Cl^- (Reuss & Weinman, 1979) crossed the basolateral membrane largely via neutral mechanisms. In contrast, Baerentsen et al. (1982) have recently concluded from model studies and the revised estimates of R_b that the conductance of the basolateral membrane is adequate to explain K^+ and Cl^- movement. Thus, consideration of distributed effects leads not only to different extracted circuit values but to qualitatively different conclusions about epithelial function.

A distributed resistor introduces a morphological parameter into an equivalent circuit model: for example, the ratio of cross-sectional area to length of the responsible structure. Thus, impedance analysis offers the possibility of estimating this morphological parameter nondestructively in the living tissue, without the problems of fixation artifacts and sampling associated with electron microscopy. In this way Clausen et al. (1979), assuming an LIS length of 20 μm in rabbit urinary bladder, used the fit of impedance data to a circuit model including a distributed resistor to estimate an LIS width of 68 Å, in the range expected from electron microscopy.

Nyquist vs. Bode Plots. Most impedance studies have represented the results as a Nyquist plot or impedance locus plot, which graphs the imaginary part of the impedance (capacitative reactance) against the real part (ohmic resistance). This method was used in all epithelial impedance studies until Clausen et al. (1979) turned to Bode plots, which graph both the phase angle and the log magnitude against log frequency. The Bode plot has three advantages: phase angle is a much more sensitive indicator of changes in circuit values than is a change in the real and imaginary parts; the linear magnitude scale of the Nyquist plot weights low-frequency data because of their high impedances; and the Nyquist plot is poorly sensitive to distributed effects because it compresses high-frequency data into a small region near the origin.

Extraction of Parameters. In fitting the circuits of Fig. 12 to epithelial impedance data, one attempts to extract values of 3–7 parameters from the data. Every physiologist is taught to suspect tail-wagging elephants whenever a model with three or more parameters is used. How can one know whether the data suffice to determine so many parameters?

This problem is one that X-ray crystallographers had to confront when they attempted to use X-ray scattering data to extract hundreds of parameters describing positions of atoms. It turns

out that, in general, the number of parameters that can be meaningfully extracted from a data set depends on the number of data points and their accuracy. A standard statistical test described by Hamilton (1964) is used to assess whether addition of each new variable to a model is significant, given the available data. With impedance measured at 25 frequencies, the data for gastric mucosa proved sufficiently accurate to warrant use of the 7-parameter model of Fig. 12*g*. Naturally, there is no assurance in advance that impedance data alone will suffice to extract values of all model parameters. For instance, in rabbit urinary bladder the time constants of the apical and basolateral membranes usually are sufficiently close that impedance data must be supplemented by direct measurement of the voltage-divider ratio to extract well determined values of all circuit parameters (Clausen et al., 1979). However, after the resistance and time constant of the apical membrane have been decreased by nystatin, a 6-parameter model can be fitted to impedance measurements in this epithelium without need of additional measurements.

Impedance Studies in Epithelia

Impedance studies in epithelia began with a bang: a pioneering paper by Teorell and Wersäll (1945) that introduced may techniques and exposed many phenomena still at the center of attention today. Using frog gastric mucosa, these authors applied frequencies sequentially, represented the data by a Nyquist plot, and used the single-*RC* model of Fig. 12 *a*. They observed changes in impedance with acid secretion, mechanical or chemical (CN^- or $CHCl_3$) damage, and K^+-Na^+ replacements. In the next year Teorell (1946) developed the alternative approach based on transient analysis and applied it to frog skin.

Three subsequent papers applied the sequential frequency method to frog skin (Brown & Kastella, 1965; Smith, 1971, 1975). The first and third of these studies were hampered by use of equivalent circuit models lacking a morphological basis (Fig. 12*a–c*), as was a study reexamining gastric mucosa around the same time (Flemström, 1971). However, Smith (1971) used a model with two *RC* subcircuits, potentially corresponding to the apical and basolateral membranes. By manipulating membrane resistance through changes in bathing salt concentration, Smith clearly resolved two time constants, corresponding to capacitance values of 1.56 and 78 μF per cm^2 chamber area. The former value was attributed to the outer facing membrane, which is only slightly folded and whose area should therefore only slightly exceed 1 cm^2 per cm^2 chamber area. To explain the high (78 μF/cm^2) value for the inner membrane, Smith reasoned that there is probably cell-to-cell coupling between the ca. five cell layers of frog skin. Thus, the effective area would be increased by a factor of 5 for the five layers, a further factor of 6 for the six faces of a cuboidal cell, and a further factor of 2 for membrane infolding.

Three papers similarly applied models with two *RC* subcircuits to gastric mucosa, of fetal rabbit (Wright, 1974) or of frog (Noyes & Rehm, 1970; Rehm et al, 1976). All three papers used the transient method and Nyquist plots. The first two of these papers separated the transient into several exponentials by graphical curve-stripping, which Rehm et al. replaced by a computer procedure. Noyes and Rehm noted that the voltage response up to 0.1 sec could be described by two exponentials, but that there were also much slower voltage changes out to 100 sec described by two further exponentials and probably reflecting changes in emf's rather than charging of membrane capacitors (Kider & Rehm, 1970). We assume that these emf changes are due to the transport number effect (Barry & Hope, 1969), and that this is why Ba^{++}, an agent known to alter gastric mucosal relative permeability coefficients and hence certain to alter the transport number effect, was found by Noyes and Rehm greatly to alter the slow phase of the transient.

These three studies made several observations that are important for understanding gastric mucosa. The fast phase of the transient could be described by two widely spaced time constants τ_1 and τ_2 (2.5 *vs.* 17, 1.5 *vs.* 17, or 0.7 *vs.* 7 m-sec in the three studies). The longer time constant τ_2 corresponded to a capacitance C_2 4–20 times the capacitance C_1 of the shorter time constant τ_1. It corresponded to a resistance R_2 2.6-fold lower than R_1 in the studies of Noyes and Rehm and of Wright, but a 2.8-fold higher resistance in the study of Rehm et al. Most important, the two capacitances related to chamber area were far higher than expected for a flat membrane (up to 2060 μF/cm^2!). As Noyes and Rehm immediately recognized, these high apparent capacitances reflect folding of the gastric mucosa at the light microscopic and electron microscopic level. Wright made the further observation that inhibition of transport by anoxia had no effect on C_1 and caused only a slight increase in R_1, but decreased C_2 several-fold while increasing R_2 several-fold. Since electron microscopy showed the apical membrane but not the basolateral membrane to decrease in area

during anoxia, Wright equated the long-τ_2 membrane with the apical membrane. However, Noyes and Rehm, Rehm et al., and Rehm and Tarvin (1978) argued that one cannot straightforwardly equate one time constant with one membrane in an epithelium consisting of multiple cell types.

Several other findings in these studies warrant mention here. Ba^{++}, which is thought to increase mucosal resistance by an effect mainly on the basolateral membrane (O'Callaghan et al., 1974), increases R_2 considerably more than R_1, contrary to Wright's reasoning. Adding high K^+ concentrations to the serosal solution decreases R_2 and C_2 by more than two-fold, R_1 and C_1 by somewhat less. (The effect of K^+ on gastric impedance was discovered by Teorell and Wersäll (1945) and was dubbed the Teorell-Wersäll effect by Rehm et al. (1976) and Ring and Sandblom (1980), although it is of minor interest compared to other effects discovered by Teorell and Wersäll in the same paper.) Finally, Rehm et al. also noted a fast time constant in the 0.1 msec range.

Distributed resistors were formulated for an epithelial circuit by Frömter (1972) and introduced to analyses of epithelial impedance data by Clausen et al. (1979). Measuring the impedance of rabbit urinary bladder by sequentially applied frequencies and depicting the results on a Bode plot, Clausen et al. detected systematic misfits to the "lumped" two membrane model of Fig. 12*d*, especially in phase angle data with increasing frequency. These misfits disappeared with the introduction of one extra parameter, the area/length ratio of the lateral intercellular spaces behaving as a distributed resistor. The extracted value of this ratio and of C for the apical and basolateral membranes agreed with electron microscopic estimates, while extracted values of R for these two membranes agreed with values obtained by cable analysis and other DC methods. Distributed models have subsequently been applied to gastric mucosa by Ring and Sandblom (1980) and Clausen et al. (1982), as will be described in the next section, and to rabbit colon by Clausen and Wills (1981).

Three important recent methodological advances in epithelial impedance studies deserve mention here, although they have not yet been applied to gastric mucosa. First, the previously discussed epithelial impedance studies used gastric mucosa, frog skin, or rabbit urinary bladder and assumed junctional conductance to be negligible, an assumption that is probably justified for these three epithelia. The more difficult problem of analyzing impedance measurements in leaky cell sheets has been attacked by Fischbarg and Lim (1973) and Rehm et al. (1973) for corneal endothelium, Schifferdecker and Frömter (1978) and Frömter et al. (1981) for *Necturus* gallbladder eipthelium, and Clausen and Wills (1981) for rabbit colon. Schifferdecker and Frömter (1978) showed that the presence of a junctional shunt makes it hard to separate the time constants of the two cell membranes by transepithelial measurements. Hence Frömter et al. (1981) introduced the measurement of epithelial impedance by an intracellular microelectrode and thereby succeeded in separating the two constants for *Necturus* gallbladder. Second, Clausen and Wills (1981) introduced the use of pseudo-random binary noise signals, in order to reduce the time required for impedance analysis far below that involved in applying frequencies sequentially without incurring the disadvantages associated with transient analysis. Both of these new approaches are likely to have widespread applicability.

Impedance Analyses of Gastric Mucosa by Distributed Models

Three papers have used distributed models to analyze impedance measurements in gastric mucosa: Ring and Sandblom (1980) and Clausen et al. (1982, 1983). We now examine the results of these studies. Both studies used frog gastric mucosa (*Rana temporaria* and *R. catesbiana,* respectively) and applied frequencies sequentially. Clausen et al. presented their data by Bode plots, while Ring and Sandblom offered both Bode plots and Nyquist plots. Ring and Sandblom used a single distributed resistor, one at the apical surface intended to model the gastric pits. Clausen et al. used two: one at the apical surface to represent either the gastric pits, or else the apical tubules and the narrow intracellular spaces between them; and one at the basolateral membrane to represent the lateral intercellular spaces.

Clausen et al. found that a lumped one-cell model (Fig. 12*d*) gave large systematic misfits to the data (Fig. 14). They then formulated a lumped two-cell model: i.e., one lacking distributed resistors, but with four *RC* subcircuits corresponding to the apical and basolateral membranes of the oxyntic cells and surface epithelial cells. This 9-parameter circuit (one series resistor, four membrane resistors, and four membrane capacitors) reduces to a 7-parameter model, six of whose parameters are complicated functions of the membrane resistors and capacitors. The fits of the model to the data were not as bad as those of the lumped

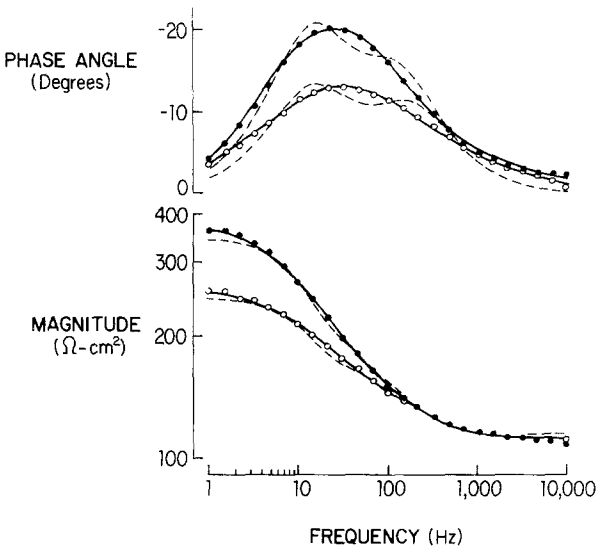

Fig. 14. Comparison of fits of lumped 1-cell ((———) and distributed (———) models to impedance measurements in a frog gastric mucosa with acid secretion inhibited by cimetidine (•) and then stimulated by histamine (o). Note that measured values at low (•) and high (o) secretion rates are very different, that the lumped model gives systematic misfits to the data (especially to the phase angle data), and that the distributed model gives good fits. The same misfits are seen with the lumped model in all experiments. The lumped 2-cell model also gives systematic misfits (not shown) somewhere less marked than those of the lumped (1-cell) model. (From Clausen, Machen, and Diamond, 1982). Copyright 1982 by the American Association for the Advancement of Science

one-cell model, but still were systematic misfits. These misfits were eliminated by the one-cell model of Fig. 12*g* with two distributed resistors, even though this model contains no more parameters than the lumped 2-cell model (Fig. 14). It may seem surprising that any type of 1-cell model works for gastric mucosa, given its multiple cell types. The reason may be that the membrane area and hence possibly the conductance of the oxyntic cells are nearly 10 times those of the surface epithelial cells. In addition, if there is lateral coupling between cell types (this question remains untested), measured properties of the apical or basolateral membrane would refer to properties averaged over the corresponding membrane of different cell types.

Both studies yielded two time constants, as had previous studies of gastric mucosa. The longer time constant, because of its higher capacitance and the variation of its capacitance with acid secretion rate, was attributed to the apical membrane, as Wright (1974) had done previously. Clausen et al. extracted the following values of C_a, R_a, C_b, and R_b from their one-cell model with two distributed resistors:

Basolateral capacitance C_b is 99 μF per cm^2 of chamber area, in good agreement with the electron microscopic measurement by Helander et al. (1972) that there are 89 cm^2 of oxyntic cell basolateral membrane area per cm^2 chamber area. The extracted C_b changes only slightly with acid secretion rate.

Apical capacitance C_a increases with increasing acid secretion rate from 200 to 8000 μF per cm^2 chamber area. This implies, as also indicated by electron microscopy, that proliferation of apical membrane area by tubulovesicles produces hundreds to thousands of cm^2 of true membrane area per cm^2 nominal area.

Basolateral resistance R_b normalized to 1 cm^2 of chamber area is 41 Ω, an absurdly low value for an epithelium. Normalized to C_b as a measure of true basolateral membrane area (1 μF ~ 1 cm^2), R_b becomes 3500 Ω μF (~3500 Ω-cm^2), a value similar to that for other tight epithelia. R_b is independent of acid secretion rate.

Transepithelial resistance normalized to 1 cm^2 chamber area is 89 Ω, an absurdly low value for a tight epithelium. Normalized to basolateral membrane area through C_b, this becomes 8800 Ω-cm^2, a value similar to that of frog skin, rabbit urinary bladder, and other tight epithelia.

Apical resistance R_a normalized to 1 cm^2 chamber area decreases from 150 to 4.6 Ω with increasing acid secretion rate, these again being absurdly low values. Normalization to apical membrane area through C_a has two effects: the apparent dependence of R_a on acid secretion rate disappears; and R_a takes on the reasonable value of 25,000 Ω-cm^2.

Thus, impedance analysis in gastric mucosa has answered two of the major puzzles of gastric electrophysiology. First, although the nominal transepithelial resistance is in the range for leaky epithelia rather than for tight epithelia, this is merely because gastric mucosa has 100 cm^2 of basolateral membrane area and perhaps up to thousands of cm^2 of apical membrane area folded into 1 cm^2 nominal area. Correction for this proliferation of area brings the transepithelial resistance into a normal range for tight epithelia, which gastric mucosa resembles in all other respects. Second, the drop in transepithelial resistance with acid secretion is due to a drop in apical resistance, which is due in turn to an increase in apical membrane area. Corrected for this increase in area, there is no change in apical resistance, hence no evidence for a change in relative permeability coefficients of the apical membrane. The change in electrical properties of gastric mucosa with acid secretion

can be fully explained by the accompanying proliferation of apical membrane area seen in the electron microscope.

It should be added, however, that this second conclusion holds only for the resting/stimulated transition of tissues bathed in normal Ringer's solutions. There are other situations in which the close relationship between apical membrane conductance and area may not hold – e.g., treatment with SCN^--containing or glucose-free solutions (Black, Forte & Forte, 1980*b*). Impedance studies of these and other physiological states may yield useful information about the control of conductance pathways in the apical and basolateral cell membranes.

Finally, we mention the analysis of Ring and Sandblom concerning the effect of K^+ on gastric impedance ("Teorell-Wersäll effect"). Parameters extracted from a lumped one-cell model show a large decrease in C_a and smaller decrease in R_b at high K^+ concentrations. The apparent decrease in C_a is at first puzzling, as K^+ is thought to stimulate acid secretion and that should increase C_a. However, the apparent decrease may be an artifact resulting from inappropriate use of a lumped model to describe an epithelium with distributed resistors. Use of a distributed model shows that the sole effect of K^+ is to decrease apical resistance, and that this effect partially masquerades as a change in C_a when one uses a lumped model. These studies by Ring and Sandblom remain to be integrated with recent morphological studies (e.g., *see* Fig. 6 of Logsdon & Machen, 1982*a*).

Unsolved Problems and Future Research

We conclude by pointing out further possible applications of impedance analysis in studies of gastric mucosa and other epithelia.

Gastric Mucosa.

1. The detailed time relations of key events in the onset of acid secretion are unclear. Is it that HCl is prepackaged in intracellular vesicles, which fuse into the apical membrane, discharge their contents, and are eventually recycled into the cell? Then the peak in acid secretion rate would precede the peak in apical capacitance but could coincide with the peak in rate of increase of apical capacitance. Is the HCl pump already running when tubular membrane is intracellular, so that HCl secretion would commence immediately as tubular membrane fused with apical membrane? Then apical capacitance and acid secretion would have the same time course. Is there a two-step process of membrane fusion followed by pump activation? Then the rise in apical capacitance would lead that in acid secretion. Recent experiments on rabbit glands, where electrical measurements have not yet been made, favor the last of these three possibilities (Gibert & Hersey, 1982).

These competing theories could be assessed by making rapid impedance measurements (e.g., by pseudorandom binary noise) to extract C_a and dC_a/dt while also measuring acid secretion.

2. How much do the gastric pits and apical tubules respectively contribute to the observed distributed effect at the apical membrane? Can the distributed effect be used to extract area-to-length estimates for the apical distributed resistor and for the lateral intercellular spaces in gastric mucosa, as has been done in rabbit urinary bladder?

3. Is there lateral coupling between oxyntic cells and surface epithelial cells, so that a one-cell model is truly appropriate? Or, are these cells not coupled, and would sufficiently accurate and abundant impedance data detect the effect of a second cell type as a deviation from fits to the one-cell distributed model?

4. There are several agents, such as K^+, Ba^{++}, and SCN^-, that are known to affect ultrastructure, electrophysiology, and acid secretion, but for which the locus of the effect is unknown or controversial. New studies of how these agents affect R_a, R_b, C_a, and C_b could be helpful in identifying their sites of action.

Other Epithelia

Applications of impedance analysis to epithelia other than gastric mucosa have been few and have yet to yield results of major physiological interest. In many epithelia, as in gastric mucosa, there are important unsolved questions involving membrane areas, conformations of long narrow membrane-bound spaces, and fusion of intracellular membrane into apical or basolateral membrane. Within the last few years four technical advances have made epithelial impedance analysis a more powerful technique than it was formerly: use of wave forms, such as pseudo-random binary noise, that offer the rapidity of transient analysis without its disadvantages; recognition of the importance of modelling distributed resistors; development of a method for intracellular impedance analysis; and development of methods for impedance analysis in leaky epthelia. The range of application for these techniques is limited only by the ingenuity of the

experimenter. As illustrations, we mention three classes of examples:

Lateral intercellular spaces distend during solute-linked fluid transport, but the dimensions of these spaces in the living epithelium are uncertain and are relevant to understanding the mechanism of fluid transport (Hill, 1975; Diamond, 1977; Spring & Hope, 1979). Distributed resistor effects arising from the lateral spaces might offer a nondestructive means of monitoring LIS width.

The pore for water permeability that ADH produces in the apical membrane of toad bladder, collecting duct, and some other tight epithelia is thought to exist intracellularly before the action of ADH, as particles visible in the electron microscope. An increase in apical capacitance as these particles are inserted into the apical membrane might offer a technique for monitoring this effect of ADH (*cf.* Wade et al., 1981). Similarly, some aldosterone-stimulated Na^+ channels in the apical membrane of rabbit urinary bladder are thought to be stored intracellularly in vesicular membrane, and insertion of this channel into the apical membrane might also be monitored as an increase in apical capacitance (Lewis & de Moura, 1982). Insertion of H^+ pumps into apical membrane of turtle bladder from cytoplasmic tubules and vesicles may be a further example (Gluck et al. 1982).

The transport of large chylomicrons from intestinal absorptive cells into the bloodstream is thought to involve exocytosis, a fusion of intracellular membrane-enclosed material into the basolateral membrane. Conversely, secretion of enzymes by the pancreas involves exocytosis of intracellular material at the apical membrane. These exocytotic mechanisms might be monitored as increases or fluctuations in the basolateral and apical capacitance, respectively.

It is a pleasure to acknowledge our debts to Chris Clausen, John Forte, and Craig Logsdon, our collaborators in much of the work reviewed here, for stimulating discussion over the years as well as for providing most of the figures. This work was supported by NIH grants AM 17328 (Center for Ulcer Research and Education), AM 19520, and GM 14772.

References

Acton, F. 1970. Numerical Methods that Work. Harper and Row, New York

Aronson, P.S. 1981. *Am. J. Physiol.* **240:***F1–F11*

Baerentsen, H.J., Christensen, O., Thomsen, P.G., Zeuthen, T. 1982. *J. Membrane Biol.* **68:**215–225

Barry, P.H., Hope, A.B. 1969. *Biophys. J.* **9:**700–728

Berglindh, T., DiBona, D.R., Pace, C.S., Sachs, G. 1980*a*. *J. Cell Biol.* **85:**392–401

Berglindh, T., DiBona, D.R., Ito, S., Sachs, G. 1980*b*. *Am. J. Physiol.* **23:***G165–G176*

Black, J.A., Forte, T.M., Forte, J.G. 1980*a*. *Anat. Rec.* **196:**163–172

Black, J.A., Forte, T.M., Forte, J.G. 1980*b*. *Fed. Proc.* **39:**377*a*

Blum, A.L., Hirschowitz, B.I., Helander, H.F., Sachs, G. 1971. *Biochim. Biophys. Acta* **241:**261–272

Brown, A.C., Kastella, K.G. 1965. *Biophys. J.* **5:**591–606

Burnham, C., Sachs, G. 1982. *Fed. Proc.* **41:**981*a*

Carrasquer, G., Chu, T., Schwartz, M., Holloman, T.L., Rehm, W.S. 1981. *Biochim. Biophys. Acta* **640:**512–520

Carrasquer, G., Chu, T.C., Schwartz, M., Rehm, W.S. 1982. *Am. J. Physiol.* **242:***G620–G627*

Chase, H.S., Al-Awqati, Q. 1981. *J. Gen. Physiol.* **77:**693–712

Chevalier, J., Bourquet, J., Hugon, J.S. 1974. *Cell Tissue Res.* **152:**129–140

Clausen, C., Fernandez, J.M. 1981. *Pfluegers Arch.* **390:**290–295

Clausen, C., Lewis, S.A., Diamond, J.M. 1979. *Biophys. J.* **26:**291–318

Clausen, C., Machen, T.E., Diamond, J.M. 1982. *Science* **217:**448–450

Clausen, C., Machen, T.E., Diamond, J.M. 1983. *Biophys. J. (in press)*

Clausen, C., Wills, N.K. 1981. *In:* Ion Transport by Epithelia. S.G. Schultz, editor. pp. 79–92. Raven Press, New York

Cole, K.S. 1972. Membranes, Ions, and Impulses. University of California Press, Berkeley

Davenport, H.W. 1962. *Proc. Soc. Exp. Biol. Med.* **110:**610–615

Davies, R.E. 1948. *Biochem. J.* **42:**609–621

Davson, H. 1964. A Textbook of General Physiology. Little Brown, Boston

Diamond, J.M. 1977. *Physiologist* **20:**10–18

Durbin, R.P., Helander, H.F. 1978. *Biochim. Biophys. Acta* **513:**179–181

Ekblad, E.B.M. 1980. *Biochim. Biophys. Acta* **632:**375–385

Fischbarg, J., Lim, J.J. 1973. *Biophys. J.* **13:**595–599

Flemström, G. 1971. *Biochim. Biophys. Acta* **225:**35–45

Flemström, G. 1977. *Am. J. Physiol.* **233:***E1–E12*

Flemström, G., Garner, A. 1982. *Am. J. Physiol.* **242:***G183–G193*

Forte, J.G., Black, J.A., Forte, T.M., Machen, T.E., Wolosin, J.M. 1982. *Am. J. Physiol.* **241:***G349–G358*

Forte, T.M., Forte, J.G. 1970. *J. Cell Biol.* **47:**782–786

Forte, T.M., Forte, J.G. 1971. *J. Ultrastr. Res.* **37:**322–334

Forte, J.G., Forte, T.M., Saltman, P. 1967. *J. Cell Physiol.* **69:**293–304

Forte, J.G., Machen, T.E. 1975. *J. Physiol. (London)* **224:**31–51

Forte, J.G., Machen, T.E. 1983. *In:* Anion Transport in Biology. G. Garrenscer, editor. Elsevier, Amsterdam (*in press*)

Forte, T.M., Machen, T.E., Forte, J.G. 1975. *Gastroenterology* **69:**1208–1222

Forte, T.M., Machen, T.E., Forte, J.G. 1977. *Gastroenterology* **73:**941–955

Forte, J.G., Machen, T.E., Öbrink, K.J. 1980. *Annu. Rev. Physiol.* **42:**111–126

Frizzell, R.A. 1976. *J. Membrane Biol.* **35:**175–187

Frizzell, R.A., Field, M., Schultz, S.G. 1978. *Am. J. Physiol.* **236:***F1–F8*

Frömter, E. 1972. *J. Membrane Biol.* **8:**259–301

Frömter, E., Diamond, J.M. 1972. *Nature New Biol.* **235:**9–13

Frömter, E., Gebler, B. 1977. *Pfluegers Arch.* **371:**99–108

Frömter, E., Suzuki, K., Kottra, G., Kampmann, L. 1981. *In:* Epithelial Ion and Water Transport. A.D.C. Macknight and J.P. Leader, editors. pp. 73–83. Raven Press, New York

Gibert, A.J., Hersey, S.J. 1982. *J. Membrane Biol.* **67:**113–124

Gluck, S., Cannon, C., Al-Awqati, Q. 1982. *Proc. Natl. Acad. Sci.* **79:**4327–4331

Grinstein, S., Erlij D. 1978. *Proc. R. Soc. London B* **202**:353–360
Gronowicz, G., Masur, S.K., Holtzman, E. 1980. *J. Membrane Biol.* **52**:221–235
Hansen, T., Slegers, J.F.G., Bonting, S.L. 1975. *Biochim. Biophys. Acta* **382**:590–608
Harmanci, M.C., Kachidorian, W.A., Valtin, H., Discala, V.A. 1978. *Am. J. Physiol.* **235**:*F*440–*F*443
Harris, J.B., Edelman, I.S. 1964. *Am. J. Physiol.* **206**:769–782
Heinz E., Durbin, R.P. 1959. *Biochim. Biophys. Acta* **31**:246–247
Helander, H.F. 1981. *Int. Res. Cytol.* **70**:279–351
Helander, H.F., Hirschowitz, B.I. 1972. *Gastroenterology* **63**:951–961
Helander, H.F., Sanders, S.S., Rehm, W.S., Hirschowitz, B.I. 1972. *In:* Gastric Secretion. G. Sachs, E. Heinz, and K.J. Ullrich, editors. pp. 69–88. Academic Press, New York
Helman, S.I., Fisher, R.S. 1977. *J. Gen. Physiol.* **69**:571–604
Hersey, S.J. 1979. *Am. J. Physiol.* **237**:*E*82–*E*89
Hersey, S.J., Chew, C.S., Campbell, L., Hopkins, E. 1981. *Am. J. Physiol.* **240**:*G*232–*G*238
Hersey, S.J., Miller, M., May, D. 1982. *Fed. Proc.* **41**:1498
Higgins, J.T., Cesaro, L., Gebler, B., Frömter, E. 1975. *Pfluegers Arch.* **358**:41–56
Hill, A.E. 1975. *Proc. R. Soc. London B* **190**:115–134
Hogben, C.A.M. 1955. *Am. J. Physiol.* **180**:641–649
Hogben, C.A.M. 1959. *Science* **129**:1224–1225
Ito, S. 1961. *J. Biophys. Biochem. Cytol.* **11**:330–347
Ito, S., Schofield, G.C. 1974. *J. Cell Biol.* **63**:364–382
Kachidorian, W.A., Muller, J., Finkelstein, A. 1981. *J. Cell Biol.* **91**:584–588
Kidder, G.W., Rehm, W.S. 1970. *Biophys. J.* **10**:215–236
Lanczos, C. 1956. Applied Analysis. Prentice Hall, Englewood Cliffs, N.J.
Lee, H.C., Breitbart, H., Berman, M., Forte, J.G. 1979. *Biochim. Biophys. Acta* **553**:107–131
Lee, H.C., Forte, J.G. 1978. *Biochim. Biophys. Acta* **508**:339–356
Lee, J., Simpson, G., Scholes, P. 1974. *Biochim. Biophys. Res. Commun.* **60**:825–829
Leeson, T.S. 1972. *Cytobiologie* **5**:352–362
Lewin, M.J.M., Ghesquier, D., Soumarmon, A., Cheret, A.M., Grelacs, F., Guesnon, J. 1977. *In:* Gastric Ion Transport. K.J. Obrink and G. Flemström, editors. pp. 267–282. Almquist and Wiksell, Stockholm
Lewis, S.A., Diamond, J.M. 1976. *J. Membrane Biol.* **28**:1–40
Lewis, S.A., Eaton, D.C., Clausen, C., Diamond, J.M. 1977. *J. Gen. Physiol.* **70**:427–440
Lewis, S.A., Eaton, D.C., Diamond, J.M. 1976. *J. Membrane Biol.* **28**:41–70
Lewis, S.A., Moura, J.L.C. de. 1982. *Nature (London)* **297**:685–688
Liedtke, C.M., Hopfer, U. 1982. *Am. J. Physiol.* **242**:*G*263–271
Loewenstein, W.R. 1981. *Physiol. Rev.* **61**:829–913
Logsdon, C.D., Machen, T.E. 1982*a*. *Am. J. Physiol.* **242**:*G*388–*G*399
Logsdon, C.D., Machen, T.E. 1982*b*. *Anat. Rec.* **202**:73–83
Machen, T.E., Forte, J.G. 1979. *In:* Membrane Transport in Biology. Vol. IV B. Transport Organs. G. Giebisch, D.C. Tosteson, and H.H. Ussing, editors. pp. 693–747. Springer, Heidelberg
Machen, T.E., McLennan, W.L. 1980. *Am. J. Physiol.* **238**:*G*403–*G*413
Machen, T.E., Silen, W., Forte, J.G. 1978. *Am. J. Physiol.* **234**:*E*228–*E*235
Machen, T.E., Zeuthen, T. 1982. *Proc. R. Soc. Ser. B.* (*in press*)
Manning, E.C., Machen, T.E. 1982. *Am. J. Physiol.* **243**:*G*60–*G*68
Manning, E.C., Machen, T.E. 1983. *Am. J. Physiol.* (*submitted*)
Mathias, R.T., Eisenberg, R.S., Valdiosera, R. 1977. *Biophys. J.* **17**:57–93
Mathias, R.T., Rae, J., Eisenberg, R.S. 1979. *Biophys. J.* **25**:181–201
McLennan, W.L., Machen, T.E., Zeuthen, T. 1980. *Am. J. Physiol.* **239**:*G*151–*G*160
Muller, J., Kachidorian, W.A., Discala, V.A. 1980. *J. Cell Biol.* **85**:83–85
Noyes, D.H., Rehm, W.S. 1970. *Am. J. Physiol.* **219**:184–192
Öbrink, K.J. 1948. *Acta Physiol. Scand.* **15(Suppl. 51)**:1–106
O'Callaghan, J., Sanders, S.S., Shoemaker, R.L., Rehm, W.S. 1974. *Am. J. Physiol.* **227**:273–288
Osawa, W., Ogata, T. 1978. *Arch. Histol. Jpn.* **41**:141–153
Rabon, E.C., Sarau, H.M., Rehm, W.S., Sachs, G. 1977. *J. Membrane Biol.*. **35**:189–204
Rabon, E., Takeguchi, N., Sachs, G. 1980. *J. Membrane Biol.* **53**:109–117
Rebolledo, I.M., Vial, J.D. 1979. *Anat. Rec.* **193**:805–822
Reenstra, W., Forte, J.G. 1981. *J. Membrane Biol.* **61**:55–60
Reenstra, W., Warnock, D., Yee, V.J., Forte, J.G. 1981. *J. Biol. Chem.* **256**:11663–11666
Rehm, W.S., Sanders, S.S. 1975. *Ann. N.Y. Acad. Sci.* **264**:442–455
Rehm, W.S., Sanders, S.S. 1977. *Gastroenterology* **73**:959–969
Rehm, W.S., Sanders, S.S., Tant, M.G., Hoffman, F.M., Tarvin, J.T. 1976. *In:* Gastric Hydrogen Secretion. D.K. Kasbekar, G. Sachs, and W.S. Rehm, editors. pp. 29–53. Dekker, New York
Rehm, W.S., Shoemaker, R.L., Sanders, S.S., Tarvin, J.T., Wright, J.A., Friday, E.A. 1973. *Exp. Eye Res.* **15**:533–552
Rehm, W.S., Tarvin, J.T. 1978. *Acta Physiol. Scand.* **Special Suppl. 1978**:143–154
Reuss, L. 1979. *J. Membrane Biol.* **47**:239–259
Reuss, L., Finn, A.L. 1974. *J. Gen. Physiol.* **64**:1–25
Reuss, L., Finn, A.L. 1975. *J. Membrane Biol.* **25**:115–139
Reuss, L., Weinman, S.A. 1979. *J. Membrane Biol.* **49**:350–362
Reuss, L., Weinman, S.A., Grady, T.P. 1980. *J. Gen. Physiol.* **76**:33–52
Ring, A., Sandblom, J. 1980. *Upsala J. Med. Sci.* **85**:283–293
Ross, I.N., Baharai, H.M.M., Turnberg, L.A. 1981. *Gastroenterology* **81**:713–718
Sachs, G., Chang, H.H., Rabon, E., Schackmann, R., Lewin, M., Saccomani, G. 1976. *J. Biol. Chem.* **251**:7690–7698
Sachs, G., Faller, L.D., Rabon, E. 1982. *J. Membrane Biol.* **64**:123–135
Sachs, G., Rabon, E., Stewart, H.B., Peerce, B., Smolka, A., Saccomani, G. 1980. *In:* Hydrogen Ion Transport in Epithelia. I. Schultz, G. Sachs, J.G. Forte, and K.J. Ullrich, editors. pp. 135–144. Elsevier, North Holland
Sachs, G., Spenney, J.G., Lewin, M. 1978. *Physiol. Rev.* **58**:106–173
Saint-Exupéry, A. de. 1943. Le Petit Prince. Harcourt, Brace, and World, New York
Schackmann, R., Schwartz, A., Saccomani, G., Sachs, G. 1977. *J. Membrane Biol.* **32**:361–381
Schettino, T., Curci, S. 1980. *Pfluegers Arch.* **383**:99–103
Schiessel, R., Merhavev, A., Matthews, J.B., Fleischer, L.A., Barzilai, A., Silen, W. 1980. *Am. J. Physiol.* **239**:*G*536–*G*542
Schifferdecker, E., Frömter, E. 1978. *Pfluegers Arch.* **377**:125–133
Schofield, G.C., Ito, S., Bolender, R.P. 1979. *J. Anat.* **128**:669–692
Schultz, S.G. 1981. *Am. J. Physiol.* **241**:*F*579–*F*590

Schwartz, M., Chu, T., Carrasquer, G., Rehm, W.S. 1981. *Biochim. Biophys. Acta* **649**:253–261
Sedar, A.W. 1969. *J. Cell Biol.* **43**:179–184
Smith, P.G. 1971. *Acta Physiol. Scand.* **81**:355–366
Smith, P.G. 1975. *Biochim. Biophys. Acta* **375**:124–129
Spangler, S.G., Rehm, W.S. 1968. *Biophys. J.* **8**:1211–1227
Spenney, J.G., Shoemaker, R.L., Sachs, G. 1974. *J. Membrane Biol.* **19**:105–128
Spring, K.R., Hope, A. 1979. *J. Gen. Physiol* **73**:287–305
Stetson, D.L., Steinmetz, P.R. 1982. *Fed. Proc.* **41**:1263a
Takeuchi, K., Silen, W. 1982. *Am. J. Physiol. (in press)*
Taylor, A. 1981. *In:* Ion Transport by Epithelia. S.G. Schultz, editor. pp. 233–259. Raven Press, New York
Taylor, A., Windhager, E.E. 1979. *Am. J. Physiol.* **236**:*F*505–512
Teorell, T. 1946. *Acta Physiol. Scand.* **12**:235–254
Teorell, T., Wersäll, R. 1945. *Acta Physiol. Scand.* **10**:243–257
Tripathi, S., Rangachari, P.K. 1980. *Am. J. Physiol.* **239**:*G*77–*G*82
Valdiosera, R., Clausen, C., Eisenberg, R.S. 1974. *J. Gen. Physiol.* **63**:432–459
Vial, J.D., Garrido, J., Dabike, M., Koenig, C. 1979. *Anat. Rec.* **194**:293–310
Voute, C.L., Möllgard, K., Ussing, H.H. 1975. *J. Membrane Biol.* **21**:273–289
Wade, J.B., Stetson, D.L., Lewis, S.A. 1981. *Ann. N.Y. Acad. Sci.* **372**:106–117
Warncke, J., Lindemann, B. 1979. *Pfluegers Arch.* **382**:*R*12
Wolosin, J.M., Forte, J.G. 1981. *J. Biol. Chem.* **256**:3149–3152
Wright, G.H. 1974. *J. Physiol. London* **242**:661–672
Wyss, J. 1814. *Swiss Family Robinson.* Godwin, London
Zeuthen, T. 1980. *In:* Transport of Ions and Water in Animals. B.L. Gupta, R.B. Moreton, J.L. Ochsman, and B.J. Well, editors. pp. 511–537. Academic Press, New York
Zimmerberg, J., Cohen, F.S., Finkelstein, A. 1980. *Science* **210**:906–908

Received 11 August 1982